Identifying genomic regions determining shoot and root traits related to nitrogen uptake efficiency in a multiparent advanced generation intercross (MAGIC) winter wheat population in a high-throughput phenotyping facility

Laura Schmidt [a], John Jacobs [b], Thomas Schmutzer [a], Ahmad M. Alqudah [c,a], Wiebke Sannemann [a,1], Klaus Pillen [a], Andreas Maurer [a,*]

[a] Martin Luther University Halle-Wittenberg, Chair of Plant Breeding, Betty-Heimann-Str. 3, 06120 Halle, Germany
[b] BASF BBCC Innovation Center Gent, 9052 Gent, Belgium
[c] Biological Science Program, Department of Biological and Environmental Sciences, College of Art and Science, Qatar University, P.O. Box 2713, Doha, Qatar

ARTICLE INFO

ABSTRACT

In the context of a continuously increasing human population that needs to be fed, with environmental protection in mind, nitrogen use efficiency (NUE) improvement is becoming very important. To understand the natural variation of traits linked to nitrogen uptake efficiency (UPE), one component of NUE, the multiparent advanced generation intercross (MAGIC) winter wheat population WM-800 was phenotyped under two contrasting nitrogen (N) levels in a high-throughput phenotyping facility for six weeks. Three biomass-related, three root-related, and two reflectance-related traits were measured weekly under each treatment. Subsequently, the population was genetically analysed using a total of 13,060 polymorphic haplotypes and singular SNPs for a genome-wide association study (GWAS). In total, we detected 543 quantitative trait loci (QTL) across all time points and traits, which were pooled into 42 stable QTL (sQTL; present in at least three of the six weeks). Besides *Rht-B1* and *Rht-D1*, candidate genes playing a role in gibberellic acid-regulated growth and nitrate transporter genes from the NPF gene family, like *NRT 1.1*, were linked to sQTL. Two novel sQTL on chromosomes 5 A and 6D showed pleiotropic effects on several traits. The high number of N-specific sQTL indicates that selection for UPE is useful specifically under N-limited conditions.

1. Introduction

Wheat is one of the most important crops for feeding the world's population. Worldwide, 19% of calories and 20% of protein intake in the human diet came from wheat in 2009 (Reynolds et al., 2012, p. 6).

Nitrogen (N) is a key actor in plant metabolism and often a limiting factor for growth, yield and quality formation in winter wheat (Hawkesford et al., 2012). Globally, 109,905,248 tons of nutrient-N were fertilized in agriculture in 2017 (on average 69.71 kg N/ha) and synthetic N-fertilizers and manure emitted 895.571 Gigagram CO2 equivalents (Food and Agriculture Organization of the United Nations, 1997). In addition to emitting greenhouse gases (Bouwman et al., 2002; Davidson, 2009), intensive N fertilization may exert negative effects on

biodiversity (Clark and Tilman, 2008; Gough et al., 2000; Suding et al., 2005) and may lead to the degradation of land and water (Diaz and Rosenberg, 2008; Guo et al., 2010).

Efficient use of N fertilizers by plants would counteract these effects. In this context, the definition of nitrogen use efficiency (NUE) established by Moll et al. (1982) can be applied in breeding. NUE is defined as produced grain dry matter yield per unit of N available in the soil, which is composed of N uptake efficiency (plant N uptake/N available N; UPE) and N utilization efficiency (grain dry matter yield/N plant uptake; UTE). Research has not yet reached a consensus on whether UPE (Baresel et al., 2008; Le Gouis et al., 2000; Liang et al., 2014) or UTE (Barraclough et al., 2010) has a greater influence on NUE under low N availability. Both parameters are subject to environmental influences

---

(Baresel et al., 2008; Guttieri et al., 2017).

Unfortunately, NUE in cereals is only about 33% worldwide (Raun and Johnson, 1999), though high-yielding sites can achieve higher NUE (Foulkes et al., 2009; Liang et al., 2014). Therefore, in addition to an effective N management strategy (Foulkes et al., 2009), breeding for increased NUE in wheat is an elementary goal in plant breeding to sustainably feed the growing world population (Hirel et al., 2007). Multiple studies showed that there is genetic variation for NUE in winter wheat (Barraclough et al., 2010; Kichey et al., 2007; Le Gouis et al., 2000) and thus there is potential for NUE improvement through breeding.

van Sanford and MacKown (1987) and Kichey et al. (2007) found that about 83% and 71.2%, respectively, of the nitrogen in the above-ground biomass at maturity was taken up by the plant before anthesis. Thus, besides post anthesis N uptake, the nitrogen uptake capacity of plants at the earlier stage plays an important role in yield and quality formation.

Plant characteristics that can contribute to the improvement of the NUE are, for instance, increased root density at depth to access water and N from deeper soil layers (King et al., 2003), enhanced root longevity post-anthesis and penetration ability of the roots (Bengough et al., 2006), decreased specific leaf N content (Semenov et al., 2007) and increased post-anthesis N uptake by plants (Triboi et al., 2006).

On the genetic level, NUE was found to be controlled by nitrate transporters of the two gene families *NRT1* (low-affinity transporter; LAT) and *NRT2* (high-affinity transporter; HAT) (Cai et al., 2008; Fraisier et al., 2000; Vidmar et al., 2000; Yin et al., 2007), which are also involved in nitrate-regulated root development (Garnett et al., 2009). Further genes described for affecting NUE are *GS1* (cytosol) and *GS2* (plastids) genes, increasing Glutamine Synthetase activity (Habash et al., 2001; Hirel et al., 2001; Martin et al., 2006; Masclaux et al., 2001), ammonium transporters of the *AMT1* gene family (Hoque et al., 2006), *ANR1* which stimulates lateral root growth in dependency of *NRT1.1* expression (Remans et al., 2006; Walch-Liu and Forde, 2008), NADH-GOGAT (Yamaya et al., 2002), *ASN1* and *ASN2* genes (Lam et al., 2003; Wong et al., 2004), *Dof1* (Kurai et al., 2011; Yanagisawa et al., 2004), glutamate receptor 1.1 (*GLR1.1*) (Kang and Turano, 2003), protein allosteric effector PII (*GLB1*) (Hsieh et al., 1998), nitrate reductase (NR) (Hänsch et al., 2001), alanine aminotransferase (*AlaAT*) (Good et al., 2007; Shrawat et al., 2008), hexose transporter *STP13* which increases expression of *NRT2.2* (Schofield et al., 2009) and the *NAC* genes (Uauy et al., 2006).

High-throughput phenotyping plays an important role in the discovery of loci and genes that affect the target trait (Al-Tamimi et al., 2016; Hickey et al., 2019). In recent years, high-throughput phenotyping methods have been successfully used for phenotyping NUE both in the greenhouse and under field conditions (Banerjee et al., 2020; Hansen et al., 2018; Jiang et al., 2019; Nguyen et al., 2019).

While mapping of quantitative trait loci (QTL) in bi-parental populations results in high statistical power, this is achieved at the expense of low genetic diversity. This problem can be circumvented by a genome-wide association study (GWAS), which allows to work with association panels consisting of genetically very diverse accessions and cultivars instead and serve as a powerful tool to dissect the genetic regulation of complex traits. However, the resulting complex population structure creates a new problem and the statistical power decreases. This is where the establishment of multi-parent advanced generation intercross (MAGIC) populations enters the field. By increasing the number of founders, it combines the advantages of the high statistical power of a bi-parental population with the high genetic diversity of association panels. In the meantime, various studies have proven the benefits of MAGIC populations for the detection of QTL in a wide variety of crops like *Arabidopsis thaliana* (Kover et al., 2009), cotton (Islam et al., 2016), barley (Sannemann et al., 2015), maize (Dell' Acqua et al., 2015), rice (Ogawa et al., 2018) and wheat (Camargo et al., 2016; Gardner et al., 2016; Huang et al., 2012; Mackay et al., 2014; Sannemann et al., 2018;

Stadlmeier et al., 2018).

To break the limitation of bi-allelic SNPs in a MAGIC population, allelic variation can be significantly increased by the approach of haplotype-based GWAS, which is based on haplotype blocks grouping two or more SNPs in strong linkage disequilibrium (LD) (Qian et al., 2017). This allows to track back the detected effects to a specific founder. Haplotype-based GWAS has already proven to be able to detect major genes as well as QTL with small effects (Chen et al., 2021; Ogawa et al., 2018; Sehgal et al., 2020).

Using the winter wheat MAGIC population WM-800 under two contrasting N levels, we investigated the genetic variation of traits that are linked to UPE and whether genotypic differences can be characterized by collecting only image-based plant growth and vitality traits using high-throughput phenotyping of young plants in a greenhouse. We conducted a haplotype-based GWAS to detect QTL controlling traits linked to UPE in WM-800, which already proved to be a valuable mapping population (Lisker et al., 2022; Sannemann et al., 2018; Schmidt et al., 2022).

2. Materials and methods

2.1. Plant material

We used WM-800, a winter wheat MAGIC population. The crossing scheme was adapted from Cavanagh et al. (2008), using eight modern German elite varieties as founders reflecting a wide range of yield potential and quality groups (Tab. S1). The population comprises 800 recombinant inbred lines in generation $F_{4:7}$, derived from intercrossing the eight founders. These lines were selected based on excluding all double-dwarf lines, carrying *Rht-B1b* and *Rht-D1b*. Previous studies already elaborated genetic characteristics of the population. The average genetic similarity (calculated based on the 27,006 polymorphic SNPs) among the founders was 0.59 with a range from 0.53 to 0.66 (Pillen et al., 2022). The 800 WM-800 lines showed an average genetic similarity of 0.60, but with a substantially increased range from 0.46 to 0.98, pointing to a high degree of genetic diversity within the population. The first and second principal component, explained 19.4% and 7.8% of the genetic similarity present in WM-800. More details on the WM-800 population are given in Sannemann et al. (2018) and Lisker et al. (2022).

2.2. Experimental set-up

The population was split into five batches due to capacity limitations, where each batch included 160 WM-800 lines, the eight founders, and four additional checks in both nitrogen treatments. After sowing, each batch of plants was grown for two weeks, vernalized for six weeks and then grown and phenotyped in the TraitMill™ high throughput phenotyping facility (Reuzeau et al., 2006) in the greenhouse for six more weeks. The weekly moving of the plants to the TraitMill™ facility resulted in reversing the order of the plants on the gutter after every phenotyping. Each genotype was represented by five biological replicates (one plant per pot per replicate) per treatment. The two nitrogen treatments were applied directly at sowing using Osmocote Exact Standard 3–4 months fertilizer containing 16% N (ICL Specialty Fertilizers, www.icl-sf.com) with 1 g/l and 4 g/l substrate for the low nitrogen treatment (N-) and the high nitrogen treatment (N+), respectively. Plants were potted in a mix of 81% peat, 9% clay and 10% ground expanded clay (0–2 mm) with an initial fertilization of Yara PG Mix 14–16–18 at 0.25 kg per m^3 in transparent, round, custom-made pots with a diameter of 12 cm and a volume of 700 ml and placed on a plant moving system.

2.3. Phenotypic data

The plants were imaged weekly in the TraitMill™ facility using an

RGB camera from the side that takes 6 pictures (at 30° angles) and an RGB camera below the plant to track root development at the bottom of the pot, together with a multispectral camera above the plant (Fig. 1). In total, eight digital traits were measured, five shoot-related traits and three root-related traits (Table 1). The RGB cameras used were Allied Vision Prosilica GT 4905 with a resolution of 0.45 mm/pixel and a field of view of 1485 × 1533 mm for the side view and a resolution of 0.036 mm/pixel and field of view of 115 × 115 mm for the root image. The top view multispectral camera was a FD-1665-MS5 Custom 3CCD Camera that used the RGB spectral bands and two additional ones at 680 nm and 808 nm with a resolution of 0.8 mm/pixel and a field of view of 860×1050 mm.

The shoot-related traits included plant area measured from a side view (PAS), plant height (HEI), gravitational height (GRA) which represents the distance along the y-axis from the base to the centre of the gravity of the plant, greenness index (GRE), and normalized difference vegetation index (NDVI). The transparency of the pots made it possible to take pictures of the root system from underneath the pots and capture the part of the root system that grew to the bottom of the pot. The root system was represented by the three traits root length (RLE), root diameter (RDI), and root area (RAR).

2.4. Statistical analyses

Data points with a median absolute deviation ≥ 3.0 from the population median were classified as outliers and removed from the data set according to Leys et al. (2013).

A linear model was fitted using the core R function "lm" with the software R (R Core Team, 2022) to test for genotype, treatment and batch effects. Genotype, treatment and batch were assigned as fixed effects and all two-way interaction effects were considered.

Data were adjusted to account for significant batch effects, detected by the linear model. In the first step, the least squares mean (LSmean) for each batch was calculated across all founders and checks over both treatments for the last phenotyping time point using the function "emmeans" (Lenth, 2020). The last time point was chosen as the standard for adjustment of all time points, because the founders there showed the highest repeatability. In the second step each value of the WM-800 lines was divided by the LSmean of founders and checks of the corresponding batch calculated in step one. In the last step, the LSmean for all founders and checks over the treatments and this time also over all batches of the last time point was calculated and each adjusted value of

Table 1
List of studied traits including name, abbreviation and description.

Trait	Abbr.	Description
Plant Area (Side View)	**PAS**	Projected plant area from a side view (in mm²)
Plant height	**HEI**	Distance (in mm) along the y-axis from base to highest point of plant
Gravitational height	**GRA**	Distance (in mm) along the y-axis from base to centre of gravity; measure for the bending of the plants
Greenness index	**GRE**	Calculated as a ratio of colour values for each plant pixel, averaged over all pixels
Normalized Difference Vegetation Index	**NDVI**	Indicator for chlorophyll content, based on difference between near-infrared (reflected by vegetation; NIR) and red light (absorbed by vegetation). NDVI is measured with a multispectral camera and calculated over each plant pixel from a top view as (NIR-Red)/(NIR+Red)
Root length	**RLE**	Projected length of all detected roots (mm)
Root diameter	**RDI**	Projected average diameter of all detected roots (mm)
Root area	**RAR**	Projected area where root biomass is detected (mm²)

the WM-800 lines was multiplied by that LSmean to re-translate the values to the original unit. After adjustment, the linear model revealed no significant batch effect anymore. A linear model was calculated again to test for genotype and treatment effects and the two-way interaction effect.

Variance components were calculated separately for the treatments with genotype modelled as a random effect, using the package "lme4″ (Bates et al., 2015) with R (R Core Team, 2022), and were used to calculate the repeatability (Rep) based on the following formula:

$$\text{Rep} = V_G/(V_G + V_R/r)$$

where V_G and V_R correspond to the variance components genotype and the residual variance, respectively and r denotes the number of replicates per genotype.

In the next step, LSmeans for all genotypes across the five replicates per treatment were calculated using the core R function "lm" and "emmeans" (Lenth, 2020) in R (R Core Team, 2022). Genotype and treatment were modelled as fixed effects.

Pearson correlation coefficients among the traits in each treatment at each time point were calculated based on the estimated LSmeans using the cor() function with R (R Core Team, 2022).

2.5. Genotypic data

The WM-800 population and the founders and checks were genetically characterized with the Infinium 15 K iSelect SNP array and the 135k Affymetrix SNP array at TraitGenetics (Gatersleben, Germany) using bulked DNA from 12 $F_{4:5}$ seedlings per WM-800 line and founder.

In total, 27,006 polymorphic SNPs (Tab. D1 in (Pillen et al., 2022)) passed the quality check which includes SNP calls for all founders, < 5% missing calls, > 5% minor allele frequency and a known physical position in the wheat genome. These polymorphic SNPs contain 7484 SNPs from the Infinium 15k iSelect array and 19,522 SNPs from the 135k Affymetrix array (given in Tab. A1 and A2 of (Pillen et al., 2022)). TraitGenetics provided the physical positions of the SNPs, anchored to the Refseq v1.1 reference genome sequence of *Triticum aestivum* (Alaux et al., 2018) for both arrays and the genetic position in centimorgan (cM) based on the wheat consensus map (Wang et al., 2014) for 7245 SNPs of the Infinium 15k iSelect array (Sannemann et al., 2018). The genetic positions for the remaining SNPs were interpolated by placing the unmapped SNPs between the two closest mapped markers based on their physical position given by (Alaux et al., 2018).

The polymorphic SNPs were transcribed into a numerical matrix based on identity by state (IBS) according to the homozygote presence
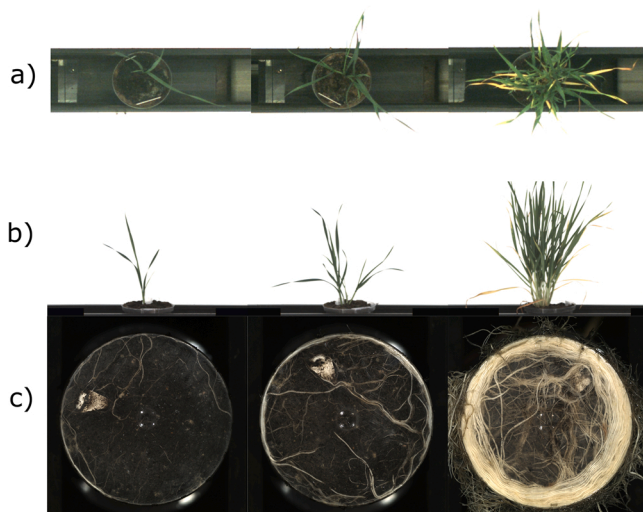

Fig. 1. : Phenotyping setup. a) Camera view from a top perspective, b) camera view from a side perspective and c) camera view from below the pot to access root parameters.

(2), heterozygote presence (1) or absence (0) of the Julius founder allele (similar as described in (Sannemann et al., 2018)) to allow regression analyses to be performed. Imputation of missing SNP calls was made based on the mean imputation (MNI) approach (Rutkoski et al., 2013).

2.6. Haplotype building

A haplotype (HT) matrix, made of SNPs in high LD, was built for WM-800 (Lisker et al., 2022) with the software package Haploview 4.2 (Barrett et al., 2005) using the SNPs of the eight founders of WM-800 and applying the 'Four Gamete Rule', that checks for SNP pairs that could not have occurred without recombination by analyzing the population frequencies of the four possible two-marker haplotypes for each SNP pair. Each SNP pair within a distance of < 500 kb was combined into a haploblock (HB) if at least one of the four possible gametes was observed with a frequency of < 0.01 and a high LD between the SNP pair was estimated with $D' = 1.0$ (Lewontin, 1964). SNPs that were not included in HBs were retained and considered "singular SNPs".

Out of 2970 HBs with a total of 92,734 HTs, 8498 informative HTs were selected as they had a HT frequency $> 5\%$ in the WM-800 population and no missing nucleotides in the HT sequence (Tab. D3 in (Pillen et al., 2022)). The selected 8498 HTs were complemented by 4562 singular SNPs. Finally, the presence of HTs and singular SNPs was then converted into a presence-absence matrix indicating 1 and 0 for the presence and absence of a specific HT in a line, respectively, to enable GWAS in a multiple linear regression framework.

2.7. GWAS

The GWAS was conducted separate for the time points and treatments with the software SAS 9.4 (SAS 9.4, 2016). In all subsequent steps the first four principle components, presented in Lisker et al. (2022), were included to correct for potential population structure effects. In the first step, all SNPs and HTs associated with the target trait were selected using a multiple linear regression model (SAS PROC GLMSELECT). This was carried out by creating 100 repeated subsamples, each containing 80% of the lines, and only those SNPs and HTs that improved the prediction of the remaining 20% were selected (according to the minimum average squared error). All SNPs and HTs selected more than one time in this step were defined as potential cofactors. The potential cofactors were then used as input for the final cofactor selection (SAS PROC GLMSELECT based on Schwarz Bayesian Criterion) in the whole dataset. The selected cofactors were then modelled with SAS PROC REG in the background of a multiple linear regression model where all SNPs and HTs were tested for significance. Thus, allele effects, the coefficient of determination (R^2) and p-value were estimated as a function of the cofactors, which entered the model first according to their ranking in the previous step, by applying the model option PARTIALR2 (SEQTESTS). Significant MTAs were merged to one QTL if they affected the same trait at the same time point and within the same treatment and if they were genetically linked within a window of < 5 cM. The effects of two linked MTAs were summed up, if at least one of them entered the regression model as a cofactor, otherwise the highest effect was taken. MTAs have been combined into stable QTL (sQTL), if they have been detected in at least three of the six phenotyping time points. Relative sQTL effects were calculated by dividing the estimated sQTL effect by the corresponding population mean. If a sQTL or two or more linked sQTL showed an effect on more than one trait they were classified as sQTL hotspots.

2.8. Candidate genes

The physical positions were anchored to the Refseq v1.1 reference genome sequence of *Triticum aestivum* (Alaux et al., 2018). The gene annotation from the IWGSC was used to identify candidate genes within the significant HB or upstream and downstream up to the neighbouring HBs. In the last step the expression profiles of candidate genes were checked using the wheat RNA-seq expression database of polyploid wheat (http://www.wheat-expression.com/).

3. Results & discussion

In WM-800, significant phenotypic differences were found among genotypes (except RLE, week five) and between N treatments (except GRA and GRE, week one) for all measured traits at p-value < 0.05, as well as significant genotype x treatment interactions (p-value < 0.001, week six) (Table 2, Tab. S2).

The initial fertilisation of the soil with Yara MPG Mix ensured a complete supply of all necessary nutrients to the plants at the start of the trial. The two treatments applied consisted of two different application rates of Osmocote, a full-spectrum fertiliser. It is therefore possible that the phenotypic differences observed between the treatments can also be attributed to nutrients other than N. However, the observed effects especially on greenness, biomass and NDVI are a strong indication that N is the critical factor, because these traits are known for their strong dependence on the N supply of the plant (Ali et al., 2020; Benincasa et al., 2018; Zhang et al., 2019).

The significant differences between the treatments as well as the significant genotype x treatment interactions indicate genotypic differences in the N use efficiency, more precisely N uptake efficiency as plants were phenotyped during vegetative growth only. N uptake efficiency was not measured directly, the traits measured in this study are to be considered as indicators reflecting the differences in N uptake efficiency between the genotypes. Especially the strong link between N uptake and NDVI and plant greenness are described in the literature (Ali et al., 2020; Benincasa et al., 2018; Jia et al., 2012), which confirms that they are suitable as an indicator for UPE.

The mean values for PAS, GRE and RDI were lower in the N- than in the N + treatment at all time points and this difference increased over time, showing that the N deficiency had a negative impact on these traits from the beginning of seedling development (Fig. 2). Serrano et al. (2000), Wang et al. (2012) and Guo et al. (2014) observed similar responses of plant growth, root growth and chlorophyll and nitrogen content to different N treatments.

In contrast, the mean values for HEI, GRA, NDVI and RAR were higher under N- than N + at the beginning of the experiment and this trend of development then reversed in the second half of the trial. A possible explanation for this observation is that under low N conditions the plants are initially sufficiently supplied by the nutrients in the grain while the plants in N + have to deal with reduced soil osmotic potential due to high mineral concentration of fertilizer which might inhibit their growth temporarily (Jacobs and Timmer, 2005). After three to four weeks this trend reverses most likely because plants under N- used up the nutrients from the kernel while the root system of the plants in N + had acclimated. RLE was the only trait that had significantly higher mean values in N- than in N + over the entire course of the trial, but the difference was only slight in week six. Increased RLE under limiting N conditions is a well-known phenomenon (Guo et al., 2014; Wang et al., 2012) and might be explained by N deficiency-induced stimulation of root development.

The WM-800 population and its founders showed moderate to high phenotypic variation, the coefficient of variation (CV %) ranged from 7.27% to 20.74% at week six for all traits except GRE, NDVI (N +) and RDI (Table 2). The CV for the WM-800 decreased over the six weeks for the traits PAS, RLE, RDI and RAR, increased for GRE and NDVI, and remained approximately constant for HEI and GRA (Tab. S2). Furthermore, the WM-800 lines showed higher variation than their founders for all traits and time points, indicating transgressive segregation. The wide range of phenotypic variation in the WM-800 population is advantageous for the selection of genetic variation in plant breeding.

Repeatability (Rep) values of WM-800 for the aboveground traits were high ($> 86\%$) in both treatments at week six. PAS was the only trait that showed a noticeable lower Rep in N- (68.40%) than in N +

Table 2

Descriptive statistics of population WM-800 and founders for eight traits measured under two N treatments after six weeks of cultivation.

Trait[a]	G[b]	T[c]	N[d]	LSmeans[e]	Min[f]	Max[g]	SD[h]	CV[i]	Rep[j]	P(G)[k]	P(T)[l]	P(GxT)[m]
PAS (mm²)	Founder	N-	8	29599	27272	34135	2302	7.78	62.67	***	***	***
		N+	8	52752	40121	60547	6478	12.28	82.24			
	WM-800	N-	799	29768	20622	39385	3127	10.50	68.40	***	***	***
		N+	793	54982	28871	76734	6768	12.31	82.17			
HEI (mm)	Founder	N-	8	476.3	323.0	598.6	85.8	18.00	93.86	***	***	***
		N+	8	531.2	389.7	627.9	82.6	15.55	86.73			
	WM-800	N-	799	507.1	274.5	838.2	105.1	20.74	92.24	***	***	***
		N+	795	573.9	223.9	879.3	117.7	20.50	91.83			
GRA (mm)	Founder	N-	8	179.9	120.2	240.2	34.8	19.36	96.80	***	***	***
		N+	8	202.0	120.0	246.2	41.7	20.62	94.90			
	WM-800	N-	797	192.9	112.7	289.8	31.5	16.34	90.62	***	***	***
		N+	794	220.1	109.0	359.5	45.5	20.65	91.78			
GRE	Founder	N-	8	1.082	1.054	1.114	0.018	1.69	88.98	***	***	***
		N+	8	1.099	1.082	1.119	0.012	1.07	82.17			
	WM-800	N-	799	1.077	1.024	1.119	0.018	1.68	87.55	***	***	***
		N+	795	1.091	1.041	1.133	0.017	1.52	90.35			
NDVI	Founder	N-	8	0.398	0.297	0.482	0.057	14.31	91.11	***	***	***
		N+	8	0.514	0.476	0.540	0.025	4.84	85.68			
	WM-800	N-	799	0.387	0.223	0.529	0.055	14.28	86.52	***	***	***
		N+	794	0.503	0.387	0.589	0.037	7.27	90.28			
RLE (mm)	Founder	N-	8	5123.6	4422.6	5535.2	372.8	7.28	52.53	***	-	**
		N+	8	5036.0	4159.2	6129.0	561.8	11.15	16.87			
	WM-800	N-	799	5001.8	3480.0	6320.3	501.1	10.02	63.22	***	***	***
		N+	760	4904.7	2457.5	6499.8	643.0	13.11	25.18			
RDI (mm)	Founder	N-	8	0.288	0.276	0.306	0.010	3.59	49.38	***	***	*
		N+	8	0.310	0.302	0.325	0.008	2.64	40.43			
	WM-800	N-	799	0.285	0.249	0.336	0.015	5.21	63.98	***	***	***
		N+	766	0.312	0.265	0.360	0.014	4.57	60.86			
RAR (mm²)	Founder	N-	8	1513.2	1246.1	1732.3	154.2	10.19	85.70	***	***	***
		N+	8	1586.1	1322.5	1996.3	210.2	13.25	92.70			
	WM-800	N-	799	1455.6	870.5	1946.5	205.9	14.14	68.50	***	***	***
		N+	763	1542.6	651.5	2157.4	229.0	14.85	36.91			

[a] Measured trait; [b] Group of genotypes; [c] Treatment: low nitrogen (N-), high nitrogen (N +); [d] Number of observations; [e] least squares means of the eight founders and the WM-800 population; [f] Minimum; [g] Maximum; [h] Standard deviation; [i] coefficient of variation (%); [j] Repeatability (%); [k] Significant differences between genotypes within N treatments; [l] Significant differences between treatments; [m] Significant genotype x treatment interaction: *p < 0.05, * *p < 0.01, * **p < 0.001. *Trait abbreviations are indicated in* Table 1.

(82.17%) (Table 2). RDI showed a moderate Rep value in both treatments in week six, while the Rep values for RLE and RAR were moderate in N- (RLE: 63.22%, RAR: 68.50%) and low in N + (RLE: 25.18%, RAR: 36.91%) treatment. Over the course of the six weeks, the Rep value decreased for PAS (N-) and all three root parameters increased for HEI and NDVI and remained relatively constant for PAS (N +), GRA and GRE (Tab. S2). These findings indicate that the above-ground traits are heritable under both N treatments while root parameters are influenced by N treatments and/or their interaction with genotype or that the method is prone to error for the scoring of root traits. Comparable values were reported for the above-ground traits (Condorelli et al., 2018; Gao et al., 2015; Mathew et al., 2018) while for root-related traits higher values have been reported (Beyer et al., 2019; Mathew et al., 2018), which might suggest an inaccuracy in measuring methods.

The Pearson correlation analysis in WM-800 revealed dynamic correlations between the eight traits over the course of the six weeks (Fig. 3). The biomass-related traits PAS, GRA, and HEI formed a block of significant positive correlations at all times. The correlations of PAS with GRA and HEI increased in the N + while they were low in the N- treatment at week six, suggesting that plants under N stress were less able to accumulate biomass over time. PAS further correlated significantly positively with RLE in both N treatments in the first four weeks. Consequently, a well-developed root system might have had a positive

effect on plant biomass development. However, the negative correlations between RLE and GRE in N + and RLE and GRA, HEI and GRE in N-, respectively, suggest that the establishment of a root system also required energy at the expense of above-ground traits. The low correlations of the traits RLE and RDI between treatments and the significant positive correlation between RLE and RDI under N- at the end of the experimental period indicated that root system development differed greatly depending on N availability. Scheible et al. (1997) described, that an accumulation of nitrate in the shoot (occurring under high N availability) inhibits root growth, whereas under N-limiting conditions root growth is promoted. RLE and RAR correlation was nearly perfect and showed similar correlations to the remaining traits, which is probably due to the fact, that RAR is a calculation based on RLE and RDI with RLE having the stronger impact due to the higher phenotypic variation.

The traits GRE and NDVI were significantly positively correlated with each other in weeks four to six. This positive correlation between spectral vegetation indices and photosynthetic pigments has been reported in multiple studies before (Kyratzis et al., 2017; Serrano et al., 2000). GRE and NDVI had significantly high negative correlations with biomass-related traits during this period. This negative correlation was also observed by Gao et al. (2015) and Liu et al. (2018) and indicates that the plants were stressed. Because both treatments behaved similarly and the negative correlations developed earlier in the N + than in the N-
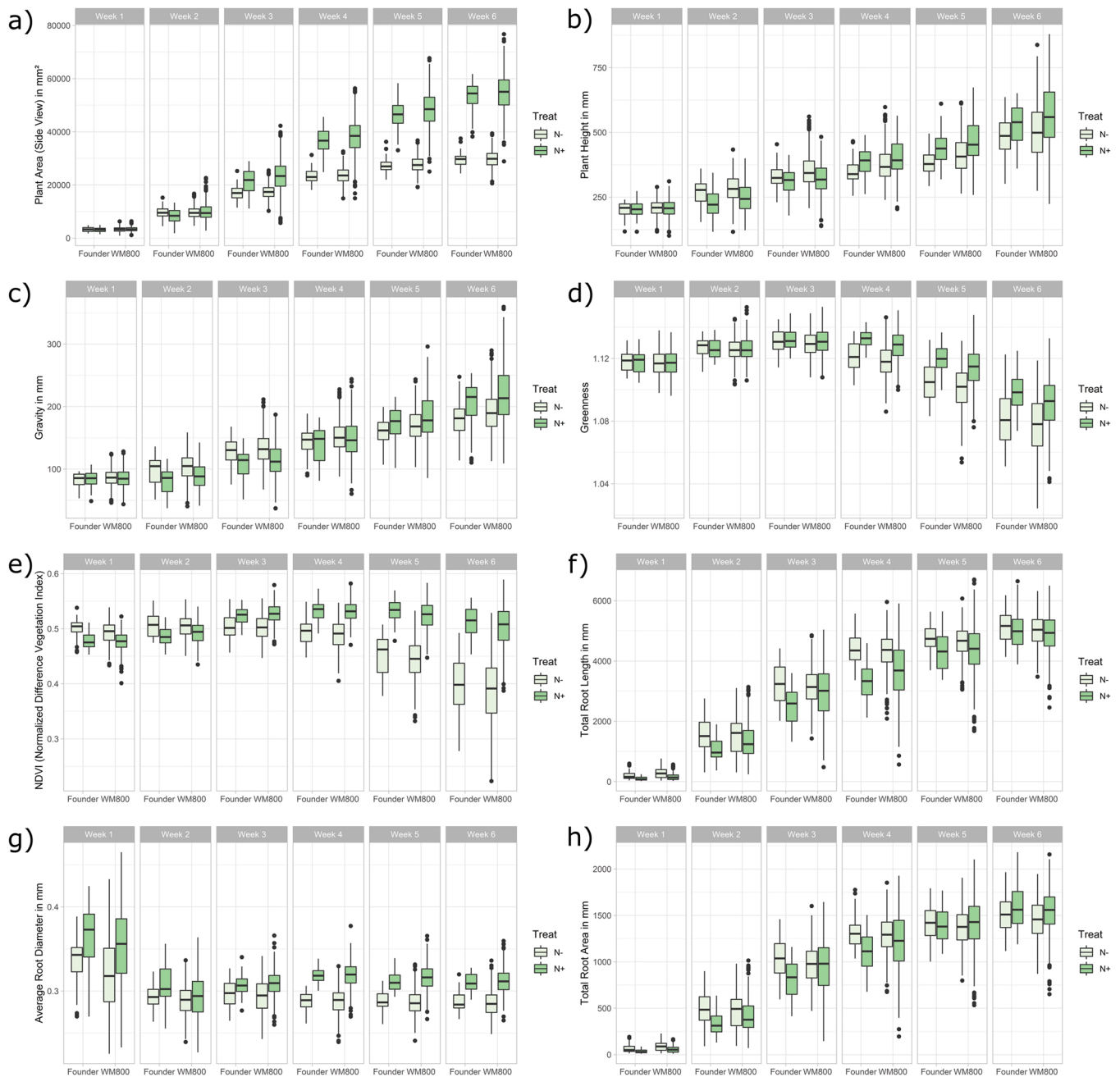
Fig. 2. : Box-Whisker-Plots indicating trait progression over six weeks per N treatment for founders and population WM-800. a) Plant area (side view) in mm^2 (PAS), b) Plant height in mm (HEI), c) Gravity in mm (GRA), d) Greenness (GRE), e) Normalized difference vegetation index (NDVI), f) Total root length in mm (RLE), g) Average root diameter in mm (RDI), h) Total root area in mm^2 (RAR).

variant, a possible explanation for the stress may be that the plants were grown in pots with limited volume. In this case, the plants may be stressed once they have entirely utilized the pot volume, which might happen earlier in N + because of a faster growth due to the sufficient N supply.

3.1. GWAS results

To investigate the genetic basis of NUE, GWAS was performed separately for each nitrogen level. First, a total of 1297 significant marker-trait associations (MTAs) (Tab. S3) were detected and the GWAS model could explain between 12.2% (RDI, N +, week four) and 69.4% (HEI, N-, week three) of the genotypic variance of a trait at one time point (Table 3). In a second step, genetically linked MTAs with a

distance < 5 cM were combined to a single QTL resulting in a total of 543 QTL. In a third step, these QTL were further combined to stable QTL per trait and treatment (sQTL), if the QTL effect was present at least during three of the six weeks of the study. This resulted in a total of 42 sQTL for the eight traits studied (Table 4) of which 14 sQTL were detected exclusively under N-, eight sQTL exclusively under N + and 20 sQTL across both N treatments (N$_{across}$). Five sQTL hotspots showed pleiotropic effects on multiple traits simultaneously, which were detected under one treatment or across both treatments. There has been a slight trend that more QTL were detected under N- than under N + or across both treatments. Along with the observation, that we detected more N-specific than N-independent QTL, this suggests that genetic regulation of these traits is differing depending on N availability and that separate selection for improved UPE under low N conditions might
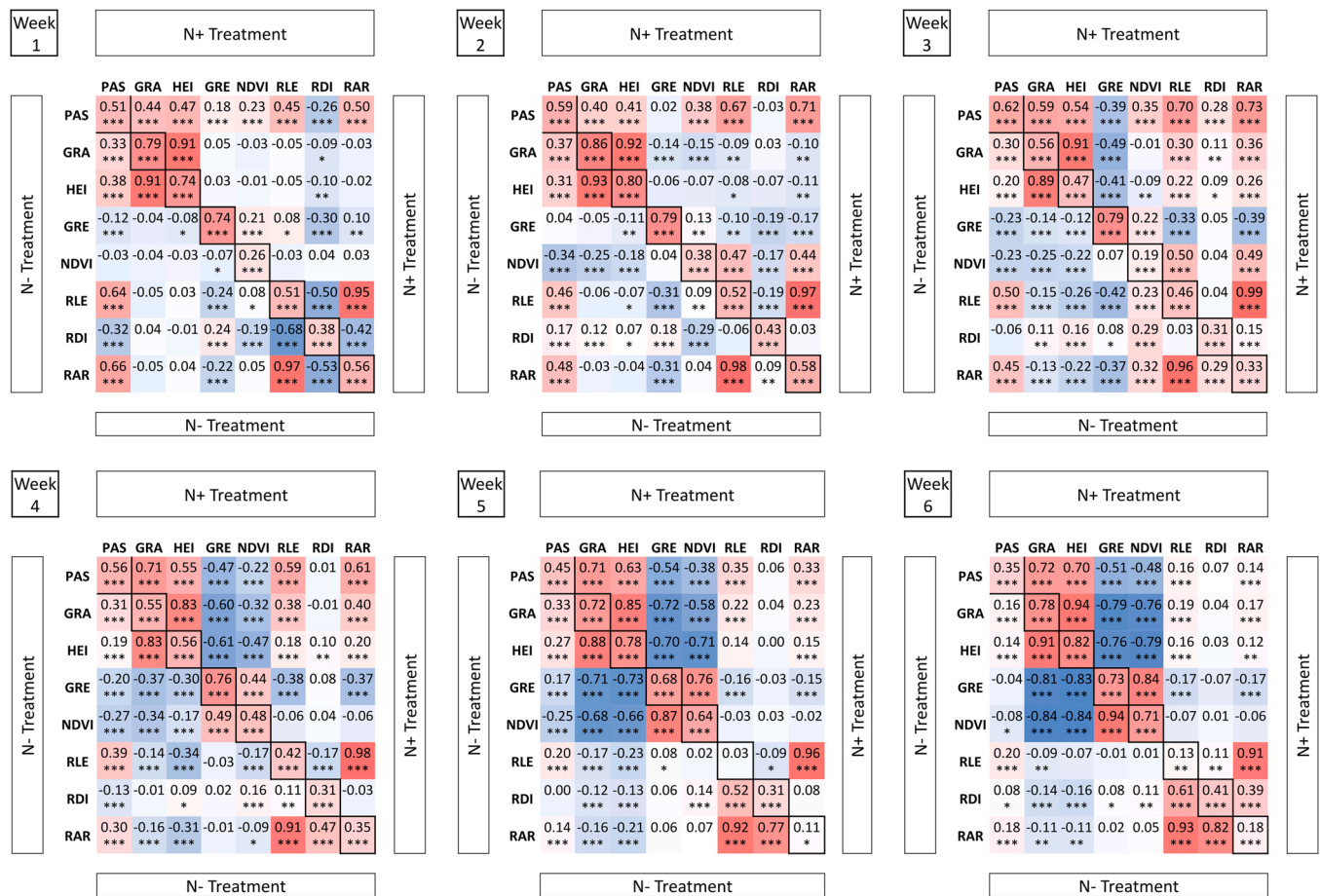
Fig. 3. : Pearson correlation tables per week of cultivation for eight traits. Upper and lower triangle represent correlation coefficients (r) under N + and N- treatments respectively. Trait auto correlations between both N treatments are indicated on the diagonal. Red and blue colours indicate positive and negative correlations, respectively. Trait abbreviations are indicated in Table 1. Significance levels: *p < 0.05, * *p < 0.01, * **p < 0.001.

be advantageous over passive selection under standard N conditions.

3.1.1. sQTL hotspots affecting multiple traits

Among the 42 sQTL, a total of 28 showed pleiotropic effects, clustering at five hotspots (Fig. 4). In the following, the five hotspots are described and discussed first and then additional sQTL of interest are added.

3.1.1.1. QTL effects derived from Rht-B1 and Rht-D1 loci.
The GWAS studies revealed two pleiotropic hotspots, that refer to QTL next to the semi-dwarf genes *Rht-B1* and *Rht-D1* on chromosomes 4B and 4D, respectively. The semi-dwarf phenotypes of alleles *Rht-B1b* and *Rht-D1b* are the results of mutations in the DELLA region of *Rht-B1* and *Rht-D1* causing the suppression of gibberellic acid (GA)-related plant growth (Peng et al., 1999). Many studies have already demonstrated that both of these *Rht* genes have pleiotropic effects on NUE and related traits (Gao et al., 2015; Gooding et al., 2012; Kubota et al., 2018).

Rht-B1 showed pleiotropic effects on HEI (sQHEI_N-_WM-800_4B & sQHEI_N+_WM-800_4B), GRA (sQGRA_N-_WM-800_4B & sQGRA_N+_WM-800_4B), GRE (sQGRE_N-_WM-800_4B & sQGRE_N+ _WM-800_4B), NDVI (sQNDVI_N-_WM-800_4B & sQNDVI_N+_WM-800_4B) and PAS N + (sQPAS_N+_WM-800_4B). The effect direction for HEI, GRA and PAS was opposite to the effect direction for GRE and NDVI across N treatments. The semi-dwarf allele *Rht-B1b* present in Tobak and Safari reduced HEI, GRA and PAS while GRE and NDVI were increased. *Rht-D1* showed pleiotropic effects on PAS, GRA, HEI, GRE and NDVI across N treatments and RAR under N- and the effect directions showed the same relation as for *Rht-B1*; when PAS, HEI and GRA showed a

positive effect, the effects for GRE, NDVI and RAR were negative (Table 4). The semi-dwarf allele *Rht-D1b* derived from Patras, Linus, JB Asano and Julius reduced PAS, HEI and GRA, while GRE, NDVI and RAR were increased. This underlines the negative relationship between biomass-related and NUE-related traits, which was already visible based on the correlations (Fig. 3). The effect of *Rht* on plant height, biomass, chlorophyll content (greenness) and NDVI was already described by others (Gao et al., 2015; Li et al., 2021; Subira et al., 2016).

The effect of *Rht-B1* was about twice as high under N + treatment than under N- treatment for GRA and HEI, while the effect on GRE and NDVI was about the same across N treatments. The QTL linked to *Rht-B1* could explain between 6.05% (PAS N +) and 19.99% (HEI N +) of the variation with a relative effect ranging from 0.29% (GRE N-) to 22.64% (HEI N +). In contrast, the QTL hotspot *Rht-D1* on 4D explained between 5.39% (RAR N-) and 26.36% (HEI N +) of the variation and had an effect on PAS (sQPAS_N-_WM-800_4D & sQPAS_N+_WM-800_4D), HEI (sQHEI_N-_WM-800_4D & sQHEI_N+_WM-800_4D), GRA (sQGRA_N-_WM-800_4D & sQGRA_N+_WM-800_4D), GRE (sQGRE_N- _WM-800_4D & sQGRE_N+_WM-800_4D), NDVI (sQNDVI_N-_WM- 800_4D & sQNDVI_N+_WM-800_4D) and RAR N- (sQRAR_N-_WM- 800_4D). The effects of the QTL showed a strong nitrogen dependency. The QTL showed markedly stronger effects under N + for GRA and PAS, while for GRE and NDVI the effects under N- were twice as high as under N + , whereas for HEI the effects showed no significant difference between the treatments.

Multiple studies showed that semi-dwarf GA insensitive genotypes have lower NUE and reduced chlorophyll content (Gooding et al., 2012; Li et al., 2018; Wang et al., 2020). In contrast, just like in our study, Gao

Table 3

Number of significant QTL, detected under N-, under N + or across treatments (N$_{across}$), explained genotypic variance (R^2) per trait, treatment and week and number of stable QTL (sQTL, detected in at least three of the six phenotyping time points) per trait and treatment.

Trait	Treat	Week 1 No. QTL	Week 1 R^2*	Week 2 No. QTL	Week 2 R^2*	Week 3 No. QTL	Week 3 R^2*	Week 4 No. QTL	Week 4 R^2*	Week 5 No. QTL	Week 5 R^2*	Week 6 No. QTL	Week 6 R^2*	No. sQTL
PAS	N-	5	40.1	5	47.5	3	34.5	4	38.4	5	37.0	2	30.9	1
	N+	6	31.0	1	31.2	6	46.0	5	44.3	5	43.7	5	48.7	3
	N$_{across}$	0		2		2		1		1		0		1
HEI	N-	2	55.1	6	59.7	12	69.4	6	65.3	1	62.5	3	66.5	2
	N+	1	56.7	1	58.6	2	46.6	1	57.3	1	65.2	5	69.3	0
	N$_{across}$	4		3		2		2		3		4		2
GRA	N-	1	58.1	3	64.4	2	61.4	3	56.1	1	60.4	2	63.5	1
	N+	2	53.5	3	62.8	7	48.3	4	57.5	3	62.1	1	65.0	1
	N$_{across}$	3		4		3		3		4		3		3
GRE	N-	6	46.3	5	50.7	7	56.6	4	54.9	3	62.3	2	57.1	0
	N+	6	37.4	5	49.9	6	50.9	4	58.4	5	53.6	3	52.2	3
	N$_{across}$	0		2		1		2		3		4		2
NDVI	N-	3	45.3	11	41.2	5	48.3	7	61.3	2	61.3	4	63.1	3
	N+	4	36.2	5	36.5	6	48.8	5	48.5	7	62.5	4	62.1	1
	N$_{across}$	0		0		3		2		3		3		2
RLE	N-	8	46.7	5	50.8	4	35.2	6	38.0	5	30.6	4	26.1	3
	N+	6	48.1	5	42.1	3	49.0	2	35.7	3	24.8	1	12.5	0
	N$_{across}$	0		0		1		0		0		0		0
RDI	N-	5	42.7	3	36.8	5	53.6	3	29.3	5	34.9	6	43.0	1
	N+	6	48.5	3	40.2	3	22.5	2	12.2	5	17.4	2	20.1	0
	N$_{across}$	0		2		0		0		0		0		0
RAR	N-	7	50.8	6	57.4	3	33.5	5	34.9	5	38.2	6	37.8	3
	N+	4	47.4	5	41.6	5	51.0	4	35.4	4	28.5	5	17.4	0
	N$_{across}$	1		0		0		0		1		0		0

* Overall percentage of genotypic variance that could be explained by the combined action of detected QTL per trait, treatment and week, including QTL which were significant across treatments and categorised as N$_{across}$. Colour variation from blue to red indicate the range from low to high R^2 values.

et al. (2015) and Shi et al. (2017) observed that semi-dwarf *Rht-B1* and *Rht-D1* alleles had a positive effect on NDVI and chlorophyll content. Yan et al. (2021) showed, that overexpression of *GA-2-oxidase* in *Arabidopsis* and maize inactivates active GAs and thus reduces plant height. Furthermore, they observed overexpression of genes involved in chlorophyll synthesis, resulting in increased chlorophyll content and reduced growth height in GA-deficient phenotypes, which support our observed effects.

3.1.1.2. Additional N-independent sQTL hotspots. A further hotspot, controlling HEI under N- (sQHEI_N-_WM-800_5A) and GRA (sQGRA_N-_WM-800_5A.2 and sQGRA_N+_WM-800_5A) across N treatments, was located on chromosome 5A between 675,386,126 and 675,731,014 bp. The QTL allele, present in Meister, JB Asano and Bernstein, reduced HEI and GRA under N- treatment by 6.31% and 8.81%, respectively, and GRA by 9.73% under N + treatment, with the treatment apparently not having a strong influence on the effect size in this case. At a very close distance to this QTL is a gene coding for a DELLA protein (IWGSC RefSeq v1.1: *TraesCS5A01G511900.1*,). DELLA proteins are negative regulators of GA signalling and thus of GA-responsive growth (Nelson and Steber, 2016). This could explain the observed effects on HEI and GRA. In a field

trial with population WM-800 under two contrasting N levels, a QTL with an effect on yield was found in close proximity to the sQTL detected here (Lisker et al., 2022). This finding indicates that QTL found in greenhouse experiments may correspond to field QTLs and may be used as a model for genetic and physiological studies on plant growth and yield formation.

A fourth hotspot was located on chromosome 6D at position 470,042,740 bp and affected RLE (N-) and PAS (N +). The Julius allele at this locus was associated with reduced RLE by − 12.50% and also PAS (N +) by − 11.19%. A potential candidate gene to explain these effects is a gene coding for a gibberellin-regulated protein (IWGSC RefSeq v1.1: *TraesCS6D02G397800.2*), which is located on chromosome 6D at position 469,391,149 bp and expressed in roots and shoots during the vegetative state. (Borrill et al., 2016; Ramírez-González et al., 2018). A hypothesis to explain the QTL effects here could be that under insufficient nitrogen supply the plants may promote root growth, while under high nitrogen supply the nutrient resources may be invested in shoot biomass development. This might happen through N-deficiency-induced growth signalling that affects the expression of the gibberellin candidate gene or upstream genes which could then result in effects on RLE under N- and PAS under N + . The physiological phenomenon of shifting

Table 4
List of 42 stable QTL (sQTL, detected in at least three of the six phenotyping time points) controlling eight traits under two N treatments in population WM-800.

Stable QTL[a]	Trait	N Treatment	Weeks	Chromosome	Start (in bp)[b]	Start (in cM)[c]	-log10 BON_p[d]	R² [%][e]	Effect Patras [%][f]	Effect Meister [%][f]	Effect Linus [%][f]	Effect JB Asano [%][f]	Effect Tobak [%][f]	Effect Safari [%][f]	Effect Bernstein [%][f]	Effect Julius [%][f]
sQPAS_N-_WM-800_1A	PAS	N-	1,4,5	1A	591,095,295	155.3	3.2	3.46	**-4.72**	**4.22**	**4.22**	**4.22**	-3.48	**4.22**	**4.22**	-1.44
sQPAS_N-_WM-800_4D	PAS	N-	2–5	4D	25,989,112	69.2	9.5	6.86	**-5.31**	**5.68**	**-5.31**	**-5.31**	**5.68**	**5.68**	**5.68**	**-5.31**
sQPAS_N+_WM-800_4B	PAS	N+	4–6	4B	30,861,580	54.6	6.8	6.05	1.45	1.67	**5.60**	1.45	**-6.75**	**-6.75**	1.67	1.67
sQPAS_N+_WM-800_4D	PAS	N+	2–6	4D	18,781,062	69.2	23.9	18.53	**-16.31**	**16.31**	**-16.31**	**-16.31**	**16.31**	**16.31**	-3.50	**-16.31**
sQPAS_N+_WM-800_5A	PAS	N+	4–6	5 A	654,389,180	112.3	5.5	4.51	**7.73**	**-7.73**	**-7.73**	**7.73**	**-7.73**	**-7.73**	**-7.73**	**-7.73**
sQPAS_N+_WM-800_6D	PAS	N+	3–5	6D	470,042,740	153.1	4.5	3.45	**11.19**	**11.19**	**11.19**	**11.19**	**11.19**	**11.19**	**11.19**	**-11.19**
sQHEI_N-_WM-800_2D	HEI	N-	3,5,6	2D	192,993,240	49.9	1.5	1.54	**-6.48**	**5.71**	**5.71**	**-6.48**	**5.71**	-1.39	**5.71**	**5.71**
sQHEI_N-_WM-800_4B	HEI	N-	1–6	4B	30,861,580	56.0	27.5	10.92	**15.53**	**15.53**	**15.53**	**15.53**	**-16.48**	**-16.48**	**15.53**	**15.53**
sQHEI_N-_WM-800_4D	HEI	N-	1–6	4D	18,781,062	69.2	29.1	19.22	**-28.81**	**29.60**	**-28.81**	**-28.81**	**29.60**	**29.60**	**29.60**	**-28.81**
sQHEI_N-_WM-800_5A	HEI	N-	1–3	5 A	675,386,126	124.1	4.6	2.73	**6.31**	**-6.31**	**6.31**	**-6.31**	**6.31**	**6.31**	**-6.31**	**6.31**
sQHEI_N+_WM-800_4B	HEI	N+	1–6	4B	30,861,580	56.0	52.0	19.99	**21.29**	**21.29**	**21.29**	**21.29**	**-22.64**	**-22.64**	**21.29**	**21.29**
sQHEI_N+_WM-800_4D	HEI	N+	1–6	4D	18,781,062	69.2	46.7	26.36	**-28.83**	**28.83**	**-28.83**	**-28.83**	**28.83**	**28.83**	**14.32**	**-28.83**
sQGRA_N-_WM-800_4B	GRA	N-	1–6	4B	30,861,580	54.6	27.4	11.10	**12.64**	**12.64**	**12.64**	**12.64**	**-12.89**	**-12.89**	**12.64**	**12.64**
sQGRA_N-_WM-800_4D	GRA	N-	1–6	4D	18,781,062	69.2	26.2	15.18	**-12.59**	**19.47**	**-12.59**	**-12.59**	**19.47**	**19.47**	**19.47**	**-12.59**
sQGRA_N-_WM-800_5A.1	GRA	N-	1,5,6	5A	590,458,527	92.0	27.1	18.01	1.86	**-24.45**	**-24.45**	**-24.45**	**-24.45**	**24.85**	**-24.45**	**-24.45**
sQGRA_N-_WM-800_5A.2	GRA	N-	1–4	5A	675,386,126	124.1	13.8	6.41	**8.81**	**-8.81**	**8.81**	**-8.81**	**8.81**	**8.81**	**-8.81**	**8.81**
sQGRA_N+_WM-800_2A	GRA	N+	2,4,5	2A	2380,829	5.9	3.9	2.50	2.55	2.72	1.84	2.55	na	0.60	1.84	**-7.78**
sQGRA_N+_WM-800_4B	GRA	N+	1–6	4B	30,861,580	56.0	47.6	19.08	**20.94**	**20.94**	**20.94**	**20.94**	**-22.46**	**-22.46**	**20.94**	**20.94**
sQGRA_N+_WM-800_4D	GRA	N+	1–6	4D	18,781,062	69.2	40.5	23.89	**-28.41**	**28.41**	**-28.41**	**-28.41**	**28.41**	**28.41**	**12.32**	**-28.41**
sQGRA_N+_WM-800_5A	GRA	N+	1–3	5A	675,386,126	124.1	4.6	3.49	**9.73**	**-9.73**	**9.73**	**-9.73**	**9.73**	**9.73**	**-9.73**	**9.73**
sQGRE_N-_WM-800_4B	GRE	N-	3–6	4B	30,861,580	54.6	13.8	8.15	-0.56	-0.29	-0.49	-0.56	**1.09**	**1.09**	-0.29	-0.29
sQGRE_N-_WM-800_4D	GRE	N-	1–6	4D	18,781,062	69.2	17.0	11.09	**1.76**	**-1.91**	**1.76**	**1.76**	**-1.91**	**-1.91**	**-1.91**	**1.76**
sQGRE_N+_WM-800_2A	GRE	N+	3–5	2A	11,846,086	26.0	4.3	2.85	0.12	**0.40**	**0.40**	**0.41**	0.12	**0.40**	**0.40**	**0.41**
sQGRE_N+_WM-800_4B	GRE	N+	4–6	4B	30,861,580	54.6	20.3	9.86	**-1.12**	**-1.12**	**-1.12**	**-1.12**	**1.22**	**1.22**	**-1.12**	**-1.12**
sQGRE_N+_WM-800_4D	GRE	N+	2–6	4D	18,781,062	69.2	14.7	8.47	**0.94**	**-0.94**	**0.94**	**0.94**	**-0.94**	**-0.94**	**-0.94**	**0.94**
sQGRE_N+_WM-800_5B	GRE	N+	3–5	5B	388,584,392	48.5	4.7	3.09	**-0.43**	**-0.43**	0.36	0.32	0.32	**-0.43**	**-0.43**	0.32

Table 4 (*continued*)

Stable QTL[a]	Trait	N Treatment	Weeks	Chromosome	Start (in bp)[b]	Start (in cM)[c]	-log10 BON_p[d]	R² [%][e]	Effect Patras [%][f]	Effect Meister [%][f]	Effect Linus [%][f]	Effect JB Asano [%][f]	Effect Tobak [%][f]	Effect Safari [%][f]	Effect Bernstein [%][f]	Effect Julius [%][f]
sQGRE_N+_WM-800_6B	GRE	N+	1,3,4,6	6B	64,118,503	47.3	2.7	2.34	**0.87**	**0.87**	**-0.87**	**0.87**	**0.87**	**0.87**	**0.87**	**0.87**
sQNDVI_N-_WM-800_4B	NDVI	N-	2–6	4B	27,838,076	53.1	14.8	6.74	**-8.58**	**-8.58**	**-8.58**	**-8.58**	**9.18**	**9.18**	**-8.58**	**-8.58**
sQNDVI_N-_WM-800_4D	NDVI	N-	3–6	4D	18,781,062	69.2	14.6	9.46	**6.37**	**-12.76**	**6.37**	**6.37**	**-12.76**	**-12.76**	**-12.76**	**6.37**
sQNDVI_N-_WM-800_5A.1	NDVI	N-	4–6	5 A	546,538,231	72.5	1.5	1.76	-2.21	0.05	-2.21	0.05	0.05	-2.21	**6.96**	-2.21
sQNDVI_N-_WM-800_5A.2	NDVI	N-	4–6	5A	594,955,076	92.6	37.6	20.13	**-11.98**	**15.41**	**15.41**	**15.41**	**15.41**	**-14.84**	**15.41**	**15.41**
sQNDVI_N-_WM-800_5D	NDVI	N-	4–6	5D	424,352,371	74.2	9.1	4.54	**-7.43**	**-7.43**	**7.43**	**-7.43**	**7.43**	**-7.43**	**-7.43**	**7.43**
sQNDVI_N+_WM-800_4B.1	NDVI	N+	3–6	4B	30,861,580	56.0	22.5	11.01	**-5.51**	**-5.51**	**-5.51**	**-5.51**	**6.30**	**6.30**	**-5.51**	**-5.51**
sQNDVI_N+_WM-800_4B.2	NDVI	N+	3–5	4B	97,922,320	62.6	2.7	2.17	**1.61**	**-1.61**	**-1.61**	**1.61**	**1.61**	**1.61**	**1.61**	**-1.61**
sQNDVI_N+_WM-800_4D	NDVI	N+	1,3–6	4D	18,781,062	69.2	28.5	15.99	**6.21**	**-6.21**	**6.21**	**6.21**	**-6.21**	**-6.21**	**-6.21**	**6.21**
sQRLE_N-_WM-800_1D	RLE	N-	1,2,4	1D	410,464,692	84.3	4.7	4.24	**5.69**	**-5.69**	**5.69**	**-5.69**	**5.69**	**5.69**	**-5.69**	**-5.69**
sQRLE_N-_WM-800_3D	RLE	N-	1,4–6	3D	43,655,074	101.1	4.0	3.83	**-4.01**	1.71	**-4.01**	1.54	**4.01**	**4.01**	**4.01**	**-4.01**
sQRLE_N-_WM-800_6D	RLE	N-	1,3,4	6D	470,042,740	153.1	4.9	4.36	**12.50**	**12.50**	**12.50**	**12.50**	**12.50**	**12.50**	**12.50**	**-12.50**
sQRDI_N-_WM-800_5A	RDI	N-	2,5,6	5A	588,023,218	90.5	2.6	2.71	**2.38**	**2.38**	**2.38**	**2.38**	**2.38**	**-2.38**	**2.38**	**2.38**
sQRAR_N-_WM-800_1B	RAR	N-	1,2,5	1B	6196,964	11.7	2.4	2.74	**7.22**	**7.22**	**7.22**	**-7.22**	**7.22**	**7.22**	**7.22**	**7.22**
sQRAR_N-_WM-800_4A	RAR	N-	1,4,5	4A	631,496,503	97.6	5.2	4.35	**6.35**	**6.35**	**6.35**	**-6.35**	**6.35**	**6.35**	**-6.35**	**-6.35**
sQRAR_N-_WM-800_4D	RAR	N-	4–6	4D	18,781,062	69.2	8.3	5.39	**7.01**	**-7.01**	**7.01**	**7.01**	**-7.01**	**-7.01**	**-7.01**	**7.01**

[c] Start of the haploblock or singular SNP, based on genetic SNP position in cM taken from (Wang et al., 2014)

[d] The -log10 Bonferroni corrected p value of significant (BON_P<0.05) haplotypes per haploblock or allele per singular SNP. Values are taken from the last week where the haplotype or singular SNP was significant.

[e] Proportion of the genotypic variance explained by significant (BON_P<0.05) haplotypes per haploblock or allele per singular SNP. Values are taken from the last week where the haplotype or singular SNP was significant.

[f] Relative sQTL effect, calculated by dividing the absolute sQTL effect by the population mean; values taken from the last week where the haplotype or singular SNP was significant. Effects of HTs that were significant in the GWAS were highlighted with bold numbers. Red colour indicates trait-reducing effects.

[a] Name of the stable QTL including information on trait, treatment, population and chromosome

[b] Start of the haploblock or singular SNP, based on physical SNP position in bp taken from (Alaux et al., 2018)
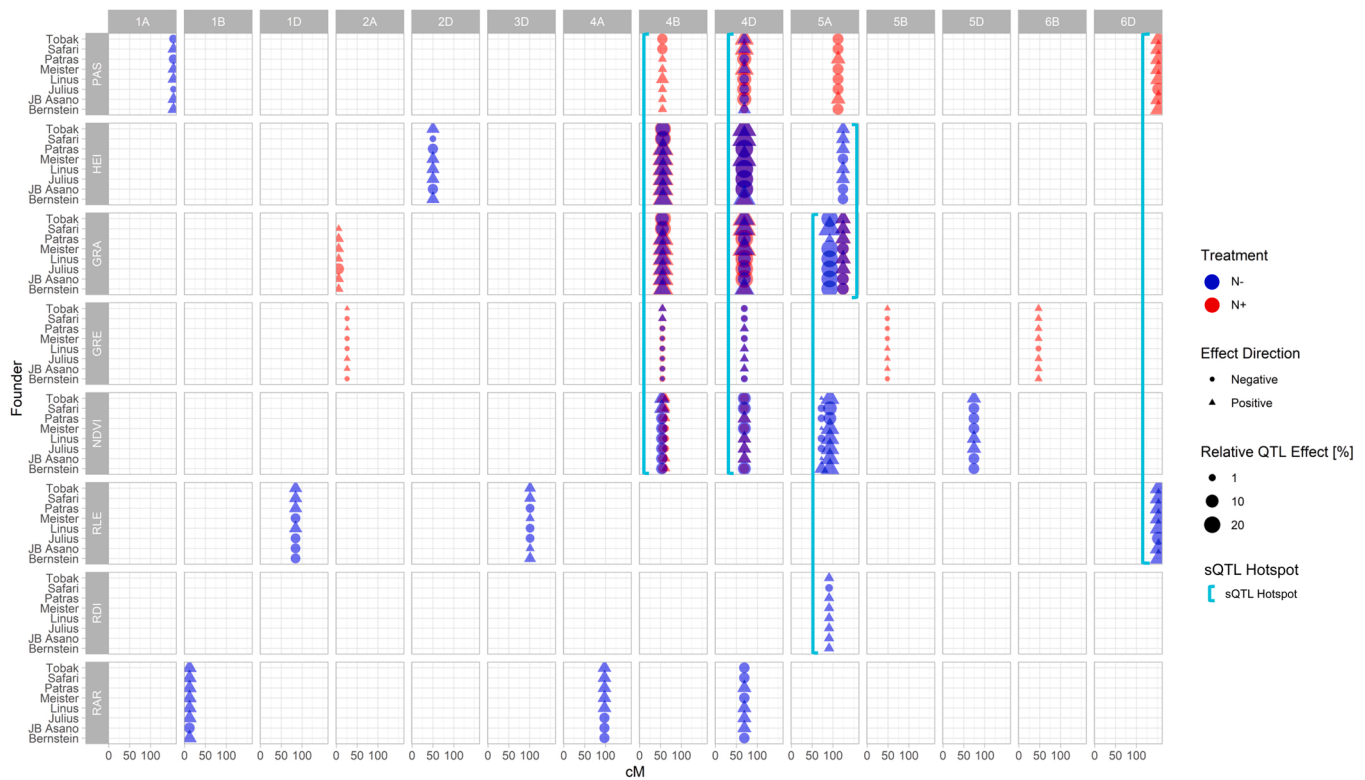
Fig. 4. : Location, direction and strength of relative stable QTL (sQTL, detected in at least three of the six phenotyping time points) allele effects in population WM-800, which are derived from eight founders. The relative effect was calculated by dividing the absolute sQTL effect by the population mean. The effects and population means were taken from the last week in which the sQTL was significant. Traits are given on the left side; trait abbreviations are indicated in Table 1.

growth between root and shoot depending on N availability was also described by Scheible et al. (1997).

3.1.1.3. N-specific QTL hotspot in close distance to NRT 1.1 and NRT 1.2.
A fifth hotspot was located on chromosome 5A between 588,023,218 and 603,380,801 bp. This hotspot revealed effects on GRA (sQGRA_N-_WM-800_5A.1), NDVI (sQNDVI_N-_WM-800_5A.2), and RDI (sQRDI_N-_WM-800_5A), which were solely detected under N- treatment (N-specific QTL). The QTL haplotype, carried by all founders except Patras and Safari, reduced GRA by 24.45% and increased NDVI and RDI by 15.41% and 2.38%, respectively. This QTL is in close proximity to two genes coding for nitrate transporters (*NRT*) *NRT1.1* and *NRT1.2* (IWGSC RefSeq v1.1: *TraesCS5A02G409600.1* and *TraesCS5A02G388000.1*, respectively). Although *NPF* family genes are known to be low-affinity transporters (Okamoto et al., 2003), Guo et al. (2014) observed that *NRT1.1* and *NRT1.2* showed increased expression under N starvation in wheat, with *NRT1.2*, in particular, showing significantly increased expression throughout the applied stress. Many studies support the assumption that *NRT1.1* functions as a dual-affinity nitrate transporter (Crawford and Glass, 1998; Liu et al., 1999; Wang et al., 1998) and it has also been found that *NRT1.1* has a crucial role as a nitrate sensor in response to N deficiency in Arabidopsis (Ho et al., 2009; Wang et al., 2012). This function may explain that the QTL has an influence on GRA and RDI in addition to NDVI. Mu et al. (2018) observed that N deficiency in maize led to a reduction of *GA20ox4*, a key enzyme for the synthesis of gibberellins, thus, reducing above-ground growth while promoting root growth. Possibly, *NRT1.1* initiated its function as a nitrate sensor also in our wheat study.

3.1.2. Biomass-related traits

3.1.2.1. Plant area from a side view (PAS). For PAS, two sQTL were detected under N- and four sQTL under N + treatments, explaining

between 3.45% and 18.53% of the genotypic variance. Only the sQTL on 4D, linked to *Rht-D1*, showed a significant effect under both treatments. The lower number of sQTL under N- is accompanied by reduced repeatabilities (as mentioned before) and R^2 values of the GWAS model over the six weeks.

3.1.2.2. Plant height (HEI). Four sQTL and two sQTL showed a significant effect on HEI under N- and N + , respectively, explaining between 1.54% and 26.36% of the variation. The sQTL on 4B, 4D and 5A have already been discussed in the preceding text as a hotspot. In addition to the hotspots, one further sQTL on 2D showed a moderate effect on HEI and was detected only under N-, with the QTL haplotype derived from Patras and JB Asano reducing HEI by 6.48%. A candidate gene could not be identified yet. While the sQTL on 4B, 4D and 5A were also detected in the field trials with the WM-800 (Lisker et al., 2022; Sannemann et al., 2018), the sQTL on 2D was not detected. This may be because plant height in our study was measured in young plants still under development whereas in the field trials the trait was measured at maturity. The sQTL on 2D, thus, may only exert an effect during early development. On the other hand, a large number of QTL for HEI were detected based on the field trials (Lisker et al., 2022; Sannemann et al., 2018), which were not detected here.

3.1.2.3. Gravitational height (GRA). For GRA, four sQTL were detected under N- and four sQTL under N + treatment. These sQTL could explain between 2.50% and 23.89% of the phenotypic variation. As for HEI, the strongest effects associated with the highest R^2 values were found for the *Rht* genes *Rht-B1* and *Rht-D1*. One sQTL on 2 A affected GRA under N + and the significant haplotype, derived from the founder Julius, reduced GRA by 7.78%. Located within this haplotype is a gene coding for a gibberellin-regulated protein (IWGSC RefSeq v1.1: *TraesCS2A02G007700.1*). A study in sorghum reported increased culm bending under gibberellin deficiency due to non-uniform cell proliferation

between the upper and lower parts of the culm internode (Ordonio et al., 2014). As GRA is a measure for the bending of the plants the observed sQTL effect may be explained by variation in the candidate gene where growth regulation is controlled downstream of gibberellin.

3.1.3. Greenness (GRE) and NDVI

3.1.3.1. Greenness (GRE). For GRE, two and five sQTL, explaining between 2.34% and 11.09% of the genotypic variation, were detected under N- and N + , respectively. The strongest effects were again estimated for the sQTL hotspots close to *Rht-B1* and *Rht-D1* on 4B and 4D. In addition to the hotspots already described, the sQTL sQGRE_N+ _WM-800_6B on 6B had a moderate effect on GRE under N + and was significant during four of the six weeks. Interestingly, close to this sQTL (at 90 Mbp) a gene is located in wheat that encodes LOW PSII ACCUMU-LATION 2 (IWGSC RefSeq v1.1: *TraesCS6B02G109300.1*). A study in Arabidopsis showed that *low psii accumulation1* mutants accumulated fewer photosystem II complexes and had altered green coloration compared to the wild type (Peng et al., 2006). A natural variation in our population for this gene could explain the observed effect on GRE but would not explain, why the effect only occurred under N + , so further research on this sQTL is necessary. A QTL in close proximity to the here described sQTL, affecting yield, was detected in the field trial with the WM-800 population independent of the N treatment (Lisker et al., 2022). Multiple studies already showed a strong linkage between the greenness of plant leaves and yield (Kanning et al., 2018; Kizilgeci et al., 2021; Rorie et al., 2011), attributable to the leaf N concentration and thus the N supply of the plant.

3.1.3.2. Normalized difference vegetation index (NDVI). For NDVI, five sQTL were detected under N- and three sQTL under N + , five of them were already described as hotspots. They could explain between 1.76% and 20.13% of the genotypic variation. *Rht-D1* explained 9.46% and 15.99% of the genotypic variance and had the strongest relative effect on NDVI with $-$ 12.76% and $-$ 6.21% under N- and N + , respectively. Apart from *Rht-D1*, the sQTL under N- showed substantially stronger effects and higher R^2 values than the sQTL under N + . The strongest sQTL, sQNDVI_N-_WM-800_5A.2, was located on 5A in close proximity to *NRT1.1* and *NRT1.2*. This QTL was detected only under N- and explained 20.13% of the variance with a relative effect of 15.41%.

The sQTL sQNDVI_N-_WM-800_5D on chromosome 5D was detected only under N-. The QTL allele present in Patras, Meister, JB Asano, Bernstein and Safari reduced NDVI by 7.43% and explained 4.54% of the variance. A candidate gene located in close proximity to this QTL encodes a light-harvesting chlorophyll a-b binding protein (LHCB) (IWGSC RefSeq v1.1: *TraesCS5D02G357600.1*), which acts as a coordinator of photosystem I and II antenna pigments with chlorophyll and xanthophyll (Jansson, 1994). Furthermore, it is well described in the literature, that the expression of *LHCB* is affected by several environmental stresses such as oxidative stress (Staneloni et al., 2008) and drought stress (Xu et al., 2012). A study in *Arabidopsis* with *LHCB* antisense mutants observed phenotypes with reduced chlorophyll content (Andersson et al., 2003). A natural variation of the expression of *LHCB* could, thus, explain the observed effect on NDVI under N deficiency stress.

The two remaining sQTL on 4B and 5A, which were significant under N+ and N-, respectively, showed minor effects with low R^2. For both sQTL no candidate genes could be determined. However, both sQTL were also detected in the WM-800 field trial with an effect on heading for the corresponding N treatment (Lisker et al., 2022). This is a strong indication of a causal link between the genetic regulation of NDVI and heading in wheat that may be investigated more closely in the future.

Many studies showed that there is a strong relationship between NDVI and yield in wheat (Duan et al., 2017; Magney et al., 2016; Raun et al., 2001). In this case, the results presented here suggest that it is useful to select for NUE under N-reduced conditions and to exploit the

effects of the N-specific QTL on, for example, 5A and 5D. Studies in maize and wheat showed that selective breeding for NUE under N deficiency conditions is more effective than indirect selection under high N conditions (Brancourt-Hulmel et al., 2005; Presterl et al., 2003).

3.1.4. Root traits

In general, for root traits less sQTL were detected than for the above-ground traits and repeatabilities and coefficient of determination values decreased over the six weeks, which is in accordance with the often reported high plasticity of roots to their environment (López-Bucio et al., 2003; Sultan, 2003). This finding may indicate that root traits were more influenced by growth conditions or measurement methods. Measuring only the roots growing to the bottom of the pot may be prone to errors because this may not perfectly account for root development inside pots. However, although this method has its weakness, the moderate to high repeatability of this trait over the six weeks suggests that there is a solid data basis for conducting a GWAS. A total of seven sQTL for root traits were detected, all of which were N- specific, suggesting that there may be potential for breeding improvement of the root system for NUE under low N availability.

3.1.4.1. Root length (RLE). For RLE, three sQTL were detected under N-, explaining between 3.83% and 4.36% of the genotypic variance. The significant haplotypes showed relative effects between 4.01% and 12.50%. In addition to the hotspot on chromosome 6D, which had the strongest effect and the highest R^2, two other sQTL on 1D and 3D showed a significant but minor effect on RLE under N-.

3.1.4.2. Root diameter (RDI). Just one sQTL showed a significant effect on RDI, detected on chromosome 5A under N-. This sQTL is close to *NRT1.1* and *NRT1.2*, already discussed as a sQTL hotspot, which explained 2.71% of the variance with a relative effect of 2.38%.

3.1.4.3. Root area (RAR). For RAR, three sQTL were detected under N-, explaining between 2.74% and 5.39% of the variance. Besides the sQTL hotspot on 4D, which is linked to *Rht-D1* and showed the strongest effect, two further sQTL on chromosomes 1B and 4A were detected. At the 1B sQTL, the haplotype derived from JB Asano reduced RAR by 7.22%. A promising candidate explaining this effect is a gene encoding the TRANSFORMING GROWTH FACTOR-BETA RECEPTOR-ASSOCIATED PROTEIN 1 (*TaTRIP1*) (IWGSC RefSeq v1.1: *TraesCS1B02G017200.2*,). In wheat, *TaTRIP1* showed significantly higher expression in genotypes with short roots than with long roots (He et al., 2014; Ren et al., 2012). They also reported, that *TaTRIP1* interacts with *TaBRI1*, encoding a brassinosteroid receptor, affecting a subset of brassinosteroid-regulated genes. Multiple studies showed that brassinosteroids regulate root growth by regulating root meristem size and cell expansion (Gao et al., 2008; Hacham et al., 2012; Li et al., 2009; Singh et al., 2016). It is also known, that brassinosteroids play an important role in abiotic stress tolerance in plants (Krishna, 2003; Ye et al., 2017) which could explain, that the described sQTL in our study was only significant under N- treatment.

The sQTL on chromosome 4A explained 4.35% of the variance with a relative effect of 6.35% under N-. This sQTL coincides with two QTL affecting yield under low N supply and grain number per ear independent of N supply, which were detected in the WM-800 population in a multi-environment field trial with two contrasting nitrogen treatments (Lisker et al., 2022). It remains open, whether there is a causal relationship between these QTL and whether a change in RAR may indeed have an impact on yield formation under low N availability.

4. Conclusion

In summary, our GWAS results indicate that a greenhouse-based high-throughput study is suitable to detect N treatment effects, N

treatment x genotype interactions and N-specific sQTL. We could show that the genetic regulation of the traits apparently depends on N availability. The haplotype-based GWAS approach allowed us to assign sQTL effects for the eight different traits to individual parents of the MAGIC population. A total of 19 sQTL were detected of which five sQTL had pleiotropic effects on multiple traits. Candidate genes besides the *Rht* genes *Rht-B1* and *Rht-D1* were genes, playing a role in GA-regulated growth and nitrate transporter genes from the NPF gene family, where in particular, the latter genes acted N treatment specific.

There has been a slight trend that more N-specific than N-independent sQTL were detected. This is an indication that genetic regulatory mechanisms of the studied traits may differ depending on N availability. Therefore, it might be more efficient to specifically select for nitrogen uptake efficiency under reduced N availability than to undertake an indirect selection for UPE under standard N conditions.

The next step to validate and better understand nitrogen uptake efficiency in the wheat population WM-800 could be the development of heterogeneous inbred families (HIFs, (Bergelson and Roux, 2010; Tuinstra et al., 1997)) from WM-800 lines that were heterozygous for the loci of interest in generation F_4. With these HIFs, QTL validation and fine mapping can subsequently be performed to ultimately clone the responsible genes for nitrogen uptake efficiency via transformation or knock-out experiments. Deciphering the genetic regulation of efficient nitrogen uptake and utilization, and selecting the relevant genes in wheat breeding programs, will allow us to support feeding the human population even with increasing requirements regarding environmental constrains and natural resource protection.

Funding

CRediT authorship contribution statement

Laura Schmidt: Formal analysis, Data curation, Writing – original draft, Visualization **John Jacobs:** Methodology, Software, Validation, Investigation, Writing – review & editing, Supervision **Thomas Schmutzer:** Data curation, Writing – review & editing **Ahmad M. Alqudah:** Writing – review & editing, Supervision **Wiebke Sannemann:** Conceptualization, Writing – review & editing, Supervision, Funding acquisition **Klaus Pillen:** Conceptualization, Writing – review & editing, Supervision, Project administration, Funding acquisition **Andreas Maurer:** Methodology, Software, Formal analysis, Writing – review & editing, Supervision.

Declaration of Competing Interest

The authors declare that they have no known competing financial interests or personal relationships that could have appeared to influence the work reported in this paper.

Data Availability

Data will be made available on request.

Acknowledgments

Appendix A. Supporting information

Supplementary data associated with this article can be found in the online version at doi:10.1016/j.plantsci.2023.111656.

References

M. Alaux, J. Rogers, T. Letellier, R. Flores, F. Alfama, C. Pommier, N. Mohellibi, S. Durand, E. Kimmel, C. Michotey, C. Guerche, M. Loaec, M. Lainé, D. Steinbach, F. Choulet, H. Rimbert, P. Leroy, N. Guilhot, J. Salse, C. Feuillet, E. Paux, K. Eversole, A.-F. Adam-Blondon, H. Quesneville, Linking the International Wheat Genome Sequencing Consortium bread wheat reference genome sequence to wheat genetic and phenomic data, Genome Biol. 19 (111) (2018), https://doi.org/10.1186/s13059-018-1491-4.

A.M. Ali, S.M. Ibrahim, Bijay-Singh, Wheat grain yield and nitrogen uptake prediction using atLeaf and GreenSeeker portable optical sensors at jointing growth stage, Inf. Process. Agric. 7 (2020) 375–383, https://doi.org/10.1016/j.inpa.2019.09.008.

N. Al-Tamimi, C. Brien, H. Oakey, B. Berger, S. Saade, Y.S. Ho, S.M. Schmöckel, M. Tester, S. Negrão, Salinity tolerance loci revealed in rice using high-throughput non-invasive phenotyping, Nat. Commun. 7 (2016) 13342, https://doi.org/10.1038/ncomms13342.

J. Andersson, M. Wentworth, R.G. Walters, C.A. Howard, A.V. Ruban, P. Horton, S. Jansson, Absence of the Lhcb1 and Lhcb2 proteins of the light-harvesting complex of photosystem II - effects on photosynthesis, grana stacking and fitness, Plant J. 35 (2003) 350–361, https://doi.org/10.1046/j.1365-313x.2003.01811.x.

B.P. Banerjee, S. Joshi, E. Thoday-Kennedy, R.K. Pasam, J. Tibbits, M. Hayden, G. Spangenberg, S. Kant, High-throughput phenotyping using digital and hyperspectral imaging-derived biomarkers for genotypic nitrogen response, J. Exp. Bot. 71 (2020) 4604–4615, https://doi.org/10.1093/jxb/eraa143.

J.P. Baresel, G. Zimmermann, H.J. Reents, Effects of genotype and environment on N uptake and N partition in organically grown winter wheat (Triticum aestivum L.) in Germany, Euphytica 163 (2008) 347–354, https://doi.org/10.1007/s10681-008-9718-1.

P.B. Barraclough, J.R. Howarth, J. Jones, R. Lopez-Bellido, S. Parmar, C.E. Shepherd, M.J. Hawkesford, Nitrogen efficiency of wheat: genotypic and environmental variation and prospects for improvement, Eur. J. Agron. 33 (2010) 1–11, https://doi.org/10.1016/j.eja.2010.01.005.

J.C. Barrett, B. Fry, J. Maller, M.J. Daly, Haploview: analysis and visualization of LD and haplotype maps, Bioinforma. (Oxf., Engl.) 21 (2005) 263–265, https://doi.org/10.1093/bioinformatics/bth457.

D. Bates, M. Mächler, B. Bolker, S. Walker, Fitting linear mixed-effects models using, lme4. J. Stat. Soft 67 (2015) 1–48, https://doi.org/10.18637/jss.v067.i01.

A.G. Bengough, M.F. Bransby, J. Hans, S.J. McKenna, T.J. Roberts, T.A. Valentine, Root responses to soil physical conditions; growth dynamics from field to cell, J. Exp. Bot. 57 (2006) 437–447, https://doi.org/10.1093/jxb/erj003.

P. Benincasa, S. Antognelli, L. Brunetti, C.A. Fabbri, A. Natale, V. Sartoretti, G. Modeo, M. Guiducci, F. Tei, M. Vizzari, Reliability of NDVI derived by high resolution satellite and UAV compared to in-field methods for the evaluation of early crop N status and grain yield in wheat, Ex. Agric. 54 (2018) 604–622, https://doi.org/10.1017/S0014479717000278.

J. Bergelson, F. Roux, Towards identifying genes underlying ecologically relevant traits in Arabidopsis thaliana, Nat. Rev. Genet. 11 (2010) 867–879, https://doi.org/10.1038/nrg2896.

S. Beyer, Daba, P. Tyagi, H. Bockelman, G. Brown-Guedira, M. Mohammadi, Loci and candidate genes controlling root traits in wheat seedlings-a wheat root GWAS, Funct. Integr. Genom. 19 (2019) 91–107, https://doi.org/10.1007/s10142-018-0630-z.

P. Borrill, R. Ramirez-Gonzalez, C. Uauy, expVIP: a customizable RNA-seq data analysis and visualization platform, Plant Physiol. 170 (2016) 2172–2186, https://doi.org/10.1104/pp.15.01667.

A.F. Bouwman, L.J.M. Boumans, N.H. Batjes, Emissions of N 2 O and NO from fertilized fields: summary of available measurement data, 16(4), 6-1-6-13. Global Biogeochem. Cycles 16, 6-1-6-13, Glob. Biogeochem. Cycles (2002), https://doi.org/10.1029/2001GB001811.

M. Brancourt-Hulmel, E. Heumez, P. Pluchard, D. Beghin, C. Depatureaux, A. Giraud, J. Gouis, Indirect versus direct selection of winter wheat for low-input or high-input levels, Crop Sci. 45 (2005) 1427–1431, https://doi.org/10.2135/cropsci2003.0343.

C. Cai, J.-Y. Wang, Y.-G. Zhu, Q.-R. Shen, B. Li, Y.-P. Tong, Z.-S. Li, Gene structure and expression of the high-affinity nitrate transport system in rice roots, J. Integr. Plant Biol. 50 (2008) 443–451, https://doi.org/10.1111/j.1744-7909.2008.00642.x.

A.V. Camargo, R. Mott, K.A. Gardner, I.J. Mackay, F. Corke, J.H. Doonan, J.T. Kim, A. R. Bentley, Determining phenological patterns associated with the onset of senescence in a wheat MAGIC mapping population, Front. Plant Sci. 7 (2016) 1540, https://doi.org/10.3389/fpls.2016.01540.

C. Cavanagh, M. Morell, I. Mackay, W. Powell, From mutations to MAGIC: resources for gene discovery, validation and delivery in crop plants, Curr. Opin. Plant Biol. 11 (2008) 215–221, https://doi.org/10.1016/j.pbi.2008.01.002.

S. Chen, F. Liu, W. Wu, Y. Jiang, K. Zhan, A SNP-based GWAS and functional haplotype-based GWAS of flag leaf-related traits and their influence on the yield of bread wheat (Triticum aestivum L.). TAG, Theor. Appl. Genet. Theor. Angew. Genet. 134 (2021) 3895–3909, https://doi.org/10.1007/s00122-021-03935-7.

C.M. Clark, D. Tilman, Loss of plant species after chronic low-level nitrogen deposition to prairie grasslands, Nature 451 (2008) 712–715, https://doi.org/10.1038/nature06503.

G.E. Condorelli, M. Maccaferri, M. Newcomb, P. Andrade-Sanchez, J.W. White, A. N. French, G. Sciara, R. Ward, R. Tuberosa, Comparative aerial and ground based high throughput phenotyping for the genetic dissection of NDVI as a proxy for drought adaptive traits in durum wheat, Front. Plant Sci. 9 (2018) 893, https://doi.org/10.3389/fpls.2018.00893.

N.M. Crawford, A.D. Glass, Molecular and physiological aspects of nitrate uptake in plants, Trends Plant Sci. 3 (1998) 389–395, https://doi.org/10.1016/S1360-1385 (98)01311-9.

E.A. Davidson, The contribution of manure and fertilizer nitrogen to atmospheric nitrous oxide since 1860, Nat. Geosci. 2 (2009) 659–662, https://doi.org/10.1038/NGEO608.

M. Dell'Acqua, D.M. Gatti, G. Pea, F. Cattonaro, F. Coppens, G. Magris, A.L. Hlaing, H. H. Aung, H. Nelissen, J. Baute, E. Frascaroli, G.A. Churchill, D. Inzé, M. Morgante, M. E. Pè, Genetic properties of the MAGIC maize population: a new platform for high definition QTL mapping in Zea mays, Genome Biol. 16 (2015) 167, https://doi.org/10.1186/s13059-015-0716-z.

R.J. Diaz, R. Rosenberg, Spreading dead zones and consequences for marine ecosystems, Sci. (N. Y., N. Y.) 321 (2008) 926–929, https://doi.org/10.1126/science.1156401.

T. Duan, S.C. Chapman, Y. Guo, B. Zheng, Dynamic monitoring of NDVI in wheat agronomy and breeding trials using an unmanned aerial vehicle, Field Crops Res. 210 (2017) 71–80, https://doi.org/10.1016/j.fcr.2017.05.025.

Food and Agriculture Organization of the United Nations, 1997. FAOSTAT Statistical Database. ⟨http://www.fao.org/faostat/en/#home⟩.

M.J. Foulkes, M.J. Hawkesford, P.B. Barraclough, M.J. Holdsworth, S. Kerr, S. Kightley, P.R. Shewry, Identifying traits to improve the nitrogen economy of wheat: recent advances and future prospects, Field Crops Res. 114 (2009) 329–342, https://doi.org/10.1016/j.fcr.2009.09.005.

V. Fraisier, A. Gojon, P. Tillard, F. Daniel-Vedele, Constitutive expression of a putative high-affinity nitrate transporter in Nicotiana plumbaginifolia: evidence for post-transcriptional regulation by a reduced nitrogen source, Plant J.: Cell Mol. Biol. 23 (2000) 489–496, https://doi.org/10.1046/j.1365-313x.2000.00813.x.

F. Gao, W. Wen, J. Liu, A. Rasheed, G. Yin, X. Xia, X. Wu, Z. He, Genome-wide linkage mapping of QTL for yield components, plant height and yield-related physiological traits in the chinese wheat cross Zhou 8425B/Chinese spring, Front. Plant Sci. 6 (2015) 1099, https://doi.org/10.3389/fpls.2015.01099.

Y. Gao, S. Wang, T. Asami, J.-G. Chen, Loss-of-function mutations in the Arabidopsis heterotrimeric G-protein alpha subunit enhance the developmental defects of brassinosteroid signaling and biosynthesis mutants, Plant Cell Physiol. 49 (2008) 1013–1024, https://doi.org/10.1093/pcp/pcn078.

K.A. Gardner, L.M. Wittern, I.J. Mackay, A highly recombined, high-density, eight-founder wheat MAGIC map reveals extensive segregation distortion and genomic locations of introgression segments, Plant Biotechnol. J. 14 (2016) 1406–1417, https://doi.org/10.1111/pbi.12504.

T. Garnett, V. Conn, B.N. Kaiser, Root based approaches to improving nitrogen use efficiency in plants, Plant, Cell Environ. (2009) 1272–1283, https://doi.org/10.1111/j.1365-3040.2009.02011.x.

A.G. Good, S.J. Johnson, M. Pauw, R.T. de, Carroll, N. Savidov, J. Vidmar, Z. Lu, G. Taylor, V. Stroeher, Engineering nitrogen use efficiency with alanine aminotransferase, Can. J. Bot. 85 (2007) 252–262, https://doi.org/10.1139/B07-019.

M.J. Gooding, M. Addisu, R.K. Uppal, J.W. Snape, H.E. Jones, Effect of wheat dwarfing genes on nitrogen-use efficiency, J. Agric. Sci. 150 (2012) 3–22, https://doi.org/10.1017/S0021859611000414.

L. Gough, C.W. Osenberg, K.L. Gross, S.L. Collins, Fertilization effects on species density and primary productivity in herbaceous plant communities, Oikos 89 (2000) 428–439, https://doi.org/10.1034/j.1600-0706.2000.890302.x.

J.H. Guo, X.J. Liu, Y. Zhang, J.L. Shen, W.X. Han, W.F. Zhang, P. Christie, K.W. T. Goulding, P.M. Vitousek, F.S. Zhang, Significant acidification in major Chinese croplands, Science 327 (2010) 1008–1010, https://doi.org/10.1126/science.1182570.

T. Guo, H. Xuan, Y. Yang, L. Wang, L. Wei, Y. Wang, G. Kang, Transcription analysis of genes encoding the wheat root transporter NRT1 and NRT2 families during nitrogen starvation, J. Plant Growth Regul. 33 (2014) 837–848, https://doi.org/10.1007/s00344-014-9435-z.

M.J. Guttieri, K. Frels, T. Regassa, B.M. Waters, P.S. Baenziger, Variation for nitrogen use efficiency traits in current and historical great plains hard winter wheat, Euphytica (2017) 213, https://doi.org/10.1007/s10681-017-1869-5.

Z. Habash, A.J. Massiah, H.L. Rong, R.M. Wallsgrove, R.A. Leigh, The role of cytosolic glutamine synthetase in wheat, Ann. Appl. Biol. 138 (2001) 83–89, https://doi.org/10.1111/j.1744-7348.2001.tb00087.x.

Y. Hacham, A. Sela, L. Friedlander, S. Savaldi-Goldstein, BRI1 activity in the root meristem involves post-transcriptional regulation of PIN auxin efflux carriers, Plant Signal. Behav. 7 (2012) 68–70, https://doi.org/10.4161/psb.7.1.18657.

R. Hänsch, D.G. Fessel, C. Witt, C. Hesberg, G. Hoffmann, P. Walch-Liu, C. Engels, J. Kruse, H. Rennenberg, W.M. Kaiser, R.-R. Mendel, Tobacco plants that lack expression of functional nitrate reductase in roots show changes in growth rates and metabolite accumulation, J. Exp. Bot. 52 (2001) 1251–1258, https://doi.org/10.1093/jexbot/52.359.1251.

N.J.S. Hansen, D. Plett, B. Berger, T. Garnett, Tackling nitrogen use efficiency in cereal crops using high-throughput phenotyping, in: A. Shrawat, A. Zayed, D.A. Lightfoot (Eds.), Engineering Nitrogen Utilization in Crop Plants. Springer International Publishing, Cham, 2018, pp. 121–139.

M. Hawkesford, W. Horst, T. Kichey, H. Lambers, J. Schjoerring, I.S. Møller, P. White, Functions of macronutrients, in: H. Marschner, P. Marschner (Eds.), Marschner's Mineral nutrition of higher plants, third ed., Elsevier Academic Press, Amsterdam, 2012, pp. 135–189.

X. He, J. Fang, J. Li, B. Qu, Y. Ren, W. Ma, X. Zhao, B. Li, D. Wang, Z. Li, Y. Tong, A genotypic difference in primary root length is associated with the inhibitory role of transforming growth factor-beta receptor-interacting protein-1 on root meristem size in wheat, Plant J. 77 (2014) 931–943, https://doi.org/10.1111/tpj.12449.

L.T. Hickey, N. Hafeez, A. Robinson, H. Jackson, S.A. Leal-Bertioli, S.C.M. Tester, M. Gao, C. Godwin, I.D. Hayes, B.J. Wulff, B.B.H, Breeding crops to feed 10 billion, Nat. Biotechnol. 37 (2019) 744–754, https://doi.org/10.1038/s41587-019-0152-9.

B. Hirel, P. Bertin, I. Quilleré, W. Bourdoncle, C. Attagnant, C. Dellay, A. Gouy, S. Cadiou, C. Retailliau, M. Falque, A. Gallais, Towards a better understanding of the genetic and physiological basis for nitrogen use efficiency in maize, Plant Physiol. 125 (2001) 1258–1270, https://doi.org/10.1104/pp.125.3.1258.

B. Hirel, J. Le Gouis, B. Ney, A. Gallais, The challenge of improving nitrogen use efficiency in crop plants: towards a more central role for genetic variability and quantitative genetics within integrated approaches, J. Exp. Bot. 58 (2007) 2369–2387, https://doi.org/10.1093/jxb/erm097.

C.-H. Ho, S.-H. Lin, H.-C. Hu, Y.-F. Tsay, CHL1 functions as a nitrate sensor in plants, Cell 138 (2009) 1184–1194, https://doi.org/10.1016/j.cell.2009.07.004.

M.S. Hoque, J. Masle, M.K. Udvardi, P.R. Ryan, N.M. Upadhyaya, Over-expression of the rice OsAMT1-1 gene increases ammonium uptake and content, but impairs growth and development of plants under high ammonium nutrition, Funct. Plant Biol.: FPB 33 (2006) 153–163, https://doi.org/10.1071/FP05165.

M.H. Hsieh, H.M. Lam, F.J. van de Loo, G. Coruzzi, A PII-like protein in Arabidopsis: putative role in nitrogen sensing, Proc. Natl. Acad. Sci. USA 95 (1998) 13965–13970, https://doi.org/10.1073/pnas.95.23.13965.

B.E. Huang, A.W. George, K.L. Forrest, A. Kilian, M.J. Hayden, M.K. Morell, C. R. Cavanagh, A multiparent advanced generation inter-cross population for genetic analysis in wheat, Plant Biotechnol. J. 10 (2012) 826–839, https://doi.org/10.1111/j.1467-7652.2012.00702.x.

M.S. Islam, G.N. Thyssen, J.N. Jenkins, L. Zeng, C.D. Delhom, J.C. McCarty, D.D. Deng, D.J. Hinchliffe, D.C. Jones, D.D. Fang, A MAGIC population-based genome-wide association study reveals functional association of GhRBB1_A07 gene with superior fiber quality in cotton, BMC Genom. 17 (2016) 903, https://doi.org/10.1186/s12864-016-3249-2.

D.F. Jacobs, V.R. Timmer, Fertilizer-induced changes in rhizosphere electrical conductivity: relation to forest tree seedling root system growth and function, New For. 30 (2005) 147–166, https://doi.org/10.1007/s11056-005-6572-z.

S. Jansson, The light-harvesting chlorophyll ab-binding proteins, Biochim. Et. Biophys. Acta (BBA) - Bioenerg. 1184 (1994) 1–19, https://doi.org/10.1016/0005-2728(94)90148-1.

L. Jia, Z. Yu, F. Li, M. Gnyp, W. Koppe, G. Bareth, Y. Miao, X. Chen, F. Zhang, Nitrogen status estimation of winter wheat by using an IKONOS satellite image in the North China Plain, in: D. Li, Y. Chen (Eds.), Computer and Computing Technologies in Agriculture V, vol. 369, Springer Berlin Heidelberg, Berlin, Heidelberg, 2012, pp. 174–184.

L. Jiang, L. Sun, M. Ye, J. Wang, Y. Wang, M. Bogard, X. Lacaze, A. Fournier, K. Beauchêne, D. Gouache, R. Wu, Functional mapping of N deficiency-induced response in wheat yield-component traits by implementing high-throughput phenotyping, Plant J (2019) 1105–1119, https://doi.org/10.1111/tpj.14186.

J. Kang, F.J. Turano, The putative glutamate receptor 1.1 (AtGLR1.1) functions as a regulator of carbon and nitrogen metabolism in Arabidopsis thaliana, Proc. Natl. Acad. Sci. USA (2003) 6872–6877, https://doi.org/10.1073/pnas.1030961100.

M. Kanning, I. Kühling, D. Trautz, T. Jarmer, High-Resolution UAV-Based Hyperspectral Imagery for LAI and Chlorophyll Estimations from Wheat for Yield Prediction, Remote Sens. 10 (2018) 2000, https://doi.org/10.3390/rs10122000.

T. Kichey, B. Hirel, E. Heumez, F. Dubois, J. Le Gouis, In winter wheat (Triticum aestivum L.), post-anthesis nitrogen uptake and remobilisation to the grain correlates with agronomic traits and nitrogen physiological markers, Field Crops Res. 102 (2007) 22–32, https://doi.org/10.1016/j.fcr.2007.01.002.

J. King, A. Gay, R. Sylvester-Bradley, I. Bingham, J. Foulkes, P. Gregory, D. Robinson, Modelling cereal root systems for water and nitrogen capture: towards an economic optimum, Ann. Bot. 91 (2003) 383–390, https://doi.org/10.1093/aob/mcg033.

F. Kizilgeci, M. Yildirim, M.S. Islam, D. Ratnasekera, M.A. Iqbal, A.E.L. Sabagh, Normalized difference vegetation index and chlorophyll content for precision nitrogen management in durum wheat cultivars under semi-arid conditions, Sustainability 13 (2021) 3725, https://doi.org/10.3390/su13073725.

P.X. Kover, W. Valdar, J. Trakalo, N. Scarcelli, I.M. Ehrenreich, M.D. Purugganan, C. Durrant, R. Mott, A multiparent advanced generation inter-cross to fine-map quantitative traits in Arabidopsis thaliana, PLoS Genet 5 (2009), e1000551, https://doi.org/10.1371/journal.pgen.1000551.

P. Krishna, Brassinosteroid-Mediated Stress Responses, J. Plant Growth Regul. 22 (2003) 289–297, https://doi.org/10.1007/s00344-003-0058-z.

H. Kubota, M. Iqbal, M. Dyck, S. Quideau, R.-C. Yang, D. Spaner, Investigating genetic progress and variation for nitrogen use efficiency in spring wheat, CSC2CROPSCI2017100598, Crop Sci. 58 (2018), https://doi.org/10.2135/cropsci2017.10.0598.

T. Kurai, M. Wakayama, T. Abiko, S. Yanagisawa, N. Aoki, R. Ohsugi, Introduction of the ZmDof1 gene into rice enhances carbon and nitrogen assimilation under low-nitrogen conditions, Plant Biotechnol. J. 9 (2011) 826–837, https://doi.org/10.1111/j.1467-7652.2011.00592.x.

A.C. Kyratzis, D.P. Skarlatos, G.C. Menexes, V.F. Vamvakousis, A. Katsiotis, Assessment of vegetation indices derived by UAV imagery for durum wheat phenotyping under a water limited and heat stressed mediterranean environment, Front. Plant Sci. 8 (2017) 1114, https://doi.org/10.3389/fpls.2017.01114.

H.-M. Lam, P. Wong, H.-K. Chan, K.-M. Yam, L. Chen, C.-M. Chow, G.M. Coruzzi, Overexpression of the ASN1 gene enhances nitrogen status in seeds of Arabidopsis, Plant Physiol. (2003) 926–935, https://doi.org/10.1104/pp.103.020123.

J. Le Gouis, D. Béghin, E. Heumez, P. Pluchard, Genetic differences for nitrogen uptake and nitrogen utilisation efficiencies in winter wheat, Eur. J. Agron. 12 (2000) 163–173, https://doi.org/10.1016/S1161-0301(00)00045-9.

Lenth, R., 2020. emmeans: Estimated Marginal Means, aka Least-Squares Means.

R.C. Lewontin, The interaction of selection and linkage. I. General considerations; heterotic models, Genetics 49 (1964) 49–67, https://doi.org/10.1093/genetics/49.1.49.

C. Leys, C. Ley, O. Klein, P. Bernard, L. Licata, Detecting outliers: Do not use standard deviation around the mean, use absolute deviation around the median, J. Exp. Soc. Psychol. 49 (2013) 764–766, https://doi.org/10.1016/j.jesp.2013.03.013.

F. Li, W. Wen, J. Liu, S. Zhai, X. Cao, C. Liu, D. Cheng, J. Guo, Y. Zi, R. Han, X. Wang, A. Liu, J. Song, J. Liu, H. Li, X. Xia, Genome-wide linkage mapping for canopy activity related traits using three RIL populations in bread wheat, Euphytica (2021) 217, https://doi.org/10.1007/s10681-021-02797-w.

J. Li, X. Mo, J. Wang, N. Chen, H. Fan, C. Dai, P. Wu, BREVIS RADIX is involved in cytokinin-mediated inhibition of lateral root initiation in Arabidopsis, Planta 229 (2009) 593–603, https://doi.org/10.1007/s00425-008-0854-6.

S. Li, Y. Tian, K. Wu, Y. Ye, J. Yu, J. Zhang, Q. Liu, M. Hu, H. Li, Y. Tong, N.P. Harberd, X. Fu, Modulating plant growth-metabolism coordination for sustainable agriculture, Nature 560 (2018) 595–600, https://doi.org/10.1038/s41586-018-0415-5.

Z. Liang, K.F. Bronson, K.R. Thorp, J. Mon, M. Badaruddin, G. Wang, Cultivar and N fertilizer rate affect yield and n use efficiency in irrigated durum wheat, Crop Sci. 54 (2014) 1175–1183, https://doi.org/10.2135/cropsci2013.03.0159.

A. Lisker, A. Maurer, T. Schmutzer, E. Kazman, H. Cöster, J. Holzapfel, E. Ebmeyer, A. M. Alqudah, W. Sannemann, K. Pillen, A haplotype-based GWAS Identified trait-improving QTL alleles controlling agronomic traits under contrasting nitrogen fertilization treatments in the MAGIC wheat population WM-800, Plants 11 (2022) 3508, https://doi.org/10.3390/plants11243508.

K.H. Liu, C.Y. Huang, Y.F. Tsay, CHL1 is a dual-affinity nitrate transporter of Arabidopsis involved in multiple phases of nitrate uptake, Plant Cell 11 (1999) 865–874, https://doi.org/10.1105/tpc.11.5.865.

Y. Liu, R. Wang, Y.-G. Hu, J. Chen, Genome-wide linkage mapping of quantitative trait loci for late-season physiological and agronomic traits in spring wheat under irrigated conditions, Agronomy 8 (2018) 60, https://doi.org/10.3390/agronomy8050060.

J. López-Bucio, A. Cruz-Ramírez, L. Herrera-Estrella, The role of nutrient availability in regulating root architecture, Curr. Opin. Plant Biol. 6 (2003) 280–287, https://doi.org/10.1016/S1369-5266(03)00035-9.

I.J. Mackay, P. Bansept-Basler, T. Barber, A.R. Bentley, J. Cockram, N. Gosman, A. J. Greenland, R. Horsnell, R. Howells, D.M. O'Sullivan, G.A. Rose, P.J. Howell, An eight-parent multiparent advanced generation inter-cross population for winter-sown wheat: creation, properties, and validation, G3 (Bethesda, Md.) 4 (2014) 1603–1610, https://doi.org/10.1534/g3.114.012963.

T.S. Magney, J.U. Eitel, D.R. Huggins, L.A. Vierling, Proximal NDVI derived phenology improves in-season predictions of wheat quantity and quality, Agric. For. Meteorol. 217 (2016) 46–60, https://doi.org/10.1016/j.agrformet.2015.11.009.

A. Martin, J. Lee, T. Kichey, D. Gerentes, M. Zivy, C. Tatout, F. Dubois, T. Balliau, B. Valot, M. Davanture, T. Tercé-Laforgue, I. Quilleré, M. Coque, A. Gallais, M.-B. Gonzalez-Moro, L. Bethencourt, D.Z. Habash, P.J. Lea, A. Charcosset, P. Perez, A. Murigneux, H. Sakakibara, K.J. Edwards, B. Hirel, Two cytosolic glutamine synthetase isoforms of maize are specifically involved in the control of grain production, Plant Cell 18 (2006) 3252–3274, https://doi.org/10.1105/tpc.106.042689.

C. Masclaux, I. Quillere, A. Gallais, B. Hirel, The challenge of remobilisation in plant nitrogen economy. A survey of physio-agronomic and molecular approaches, Ann. Appl. Biol. 138 (2001) 69–81, https://doi.org/10.1111/j.1744-7348.2001.tb00086.x.

I. Mathew, H. Shimelis, L. Mwadzingeni, R. Zengeni, M. Mutema, V. Chaplot, Variance components and heritability of traits related to root: shoot biomass allocation and drought tolerance in wheat, Euphytica (2018) 214, https://doi.org/10.1007/s10681-018-2302-4.

R.H. Moll, E.J. Kamprath, W.A. Jackson, Analysis and interpretation of factors which contribute to efficiency of nitrogen utilization 1, Agron. J. 74 (1982) 562–564, https://doi.org/10.2134/agronj1982.00021962007400030037x.

X. Mu, Q. Chen, X. Wu, F. Chen, L. Yuan, G. Mi, Gibberellins synthesis is involved in the reduction of cell flux and elemental growth rate in maize leaf under low nitrogen supply, Environ. Exp. Bot. 150 (2018) 198–208, https://doi.org/10.1016/j.envexpbot.2018.03.012.

S.K. Nelson, C.M. Steber, Gibberellin hormone signal perception: down-regulating DELLA repressors of plant growth and development, in: P. Hedden, S.G. Thomas (Eds.), Annual Plant Reviews, The Gibberellins, 1st ed., Wiley-Blackwell, 2016, pp. 153–188.

G.N. Nguyen, P. Maharjan, L. Maphosa, J. Vakani, E. Thoday-Kennedy, S. Kant, A robust automated image-based phenotyping method for rapid vegetative screening of wheat germplasm for nitrogen use efficiency, Front. Plant Sci. 10 (2019) 1372, https://doi.org/10.3389/fpls.2019.01372.

D. Ogawa, Y. Nonoue, H. Tsunematsu, N. Kanno, T. Yamamoto, J. Yonemaru, Discovery of QTL alleles for grain shape in the japan-MAGIC rice population using haplotype information, G3 Bethesda Md. 8 (2018) 3559–3565, https://doi.org/10.1534/g3.118.200558.

M. Okamoto, J.J. Vidmar, A.D.M. Glass, Regulation of NRT1 and NRT2 gene families of Arabidopsis thaliana: responses to nitrate provision, Plant Cell Physiol. 44 (2003) 304–317, https://doi.org/10.1093/pcp/pcg036.

R.L. Ordonio, Y. Ito, A. Hatakeyama, K. Ohmae-Shinohara, S. Kasuga, T. Tokunaga, H. Mizuno, H. Kitano, M. Matsuoka, T. Sazuka, Gibberellin deficiency pleiotropically

induces culm bending in sorghum: an insight into sorghum semi-dwarf breeding, Sci. Rep. 4 (2014) 5287, https://doi.org/10.1038/srep05287.

J. Peng, D.E. Richards, N.M. Hartley, G.P. Murphy, K.M. Devos, J.E. Flintham, J. Beales, L.J. Fish, A.J. Worland, F. Pelica, D. Sudhakar, P. Christou, J.W. Snape, M.D. Gale, N. P. Harberd, 'Green revolution' genes encode mutant gibberellin response modulators, Nature 400 (1999) 256–261, https://doi.org/10.1038/22307.

L. Peng, J. Ma, W. Chi, J. Guo, S. Zhu, Q. Lu, C. Lu, L. Zhang, LOW PSII ACCUMULATION1 is involved in efficient assembly of photosystem II in Arabidopsis thaliana, Plant Cell 18 (2006) 955–969, https://doi.org/10.1105/tpc.105.037689.

Pillen, K., Sannemann, W., Lisker, A., Maurer, A., Schmutzer, T., Alqudah, A.M., 2022. Determining haploblocks and haplotypes in the MAGIC winter wheat population WM-800 based on the wheat 15k Infinium and the 135k Affymetrix SNP arrays.

T. Presterl, G. Seitz, M. Landbeck, E.M. Thiemt, W. Schmidt, H.H. Geiger, Improving nitrogen-use efficiency in european maize, Crop Sci. 43 (2003) 1259–1265, https://doi.org/10.2135/cropsci2003.1259.

L. Qian, L.T. Hickey, A. Stahl, C.R. Werner, B. Hayes, R.J. Snowdon, K.P. Voss-Fels, Exploring and harnessing haplotype diversity to improve yield stability in crops, Front. Plant Sci. 8 (2017) 1534, https://doi.org/10.3389/fpls.2017.01534.

R Core Team, 2022. R: A Language and Environment for Statistical Computing. R Foundation for Statistical Computing, Vienna, Austria, Vienna, Austria.

R.H. Ramírez-González, P. Borrill, D. Lang, S.A. Harrington, J. Brinton, L. Venturini, M. Davey, J. Jacobs, F. van Ex, A. Pasha, Y. Khedikar, S.J. Robinson, A.T. Cory, T. Florio, L. Concia, C. Juery, H. Schoonbeek, B. Steuernagel, D. Xiang, C.J. Ridout, B. Chalhoub, K.F.X. Mayer, M. Benhamed, D. Latrasse, A. Bendahmane, B.B.H. Wulff, R. Appels, V. Tiwari, R. Datla, F. Choulet, C.J. Pozniak, N.J. Provart, A.G. Sharpe, E. Paux, M. Spannagl, A. Bräutigam, C. Uauy, The transcriptional landscape of polyploid wheat, Sci. (N. Y., N. Y.) 361 (2018), https://doi.org/10.1126/science.aar6089.

W.R. Raun, G.V. Johnson, Improving nitrogen use efficiency for cereal production, Agron. J. 91 (1999) 357–363, https://doi.org/10.2134/AGRONJ1999.00021962009100030001X.

W.R. Raun, J.B. Solie, G.V. Johnson, M.L. Stone, E.V. Lukina, W.E. Thomason, J. S. Schepers, In-season prediction of potential grain yield in winter wheat using canopy reflectance, Agron. J. 93 (2001) 131–138, https://doi.org/10.2134/agronj.931131x.

T. Remans, P. Nacry, M. Pervent, S. Filleur, E. Diatloff, E. Mounier, P. Tillard, B.G. Forde, A. Gojon, The Arabidopsis NRT1.1 transporter participates in the signaling pathway triggering root colonization of nitrate-rich patches, Proc. Natl. Acad. Sci. USA 103 (2006) 19206–19211, https://doi.org/10.1073/pnas.0605275103.

Y. Ren, X. He, D. Liu, J. Li, X. Zhao, B. Li, Y. Tong, A. Zhang, Z. Li, Major quantitative trait loci for seminal root morphology of wheat seedlings, Mol. Breed. 30 (2012) 139–148, https://doi.org/10.1007/s11032-011-9605-7.

C. Reuzeau, V. Frankard, Y. Hatzfeld, A. Sanz, W. van Camp, P. Lejeune, C. Wilde, K. de, Lievens, J. Wolf, E. de, Vranken, R. Peerbolte, W. Broekaert, Traitmill™: a functional genomics platform for the phenotypic analysis of cereals, Plant Genet. Resour. 4 (2006) 20–24, https://doi.org/10.1079/PGR2005104.

Reynolds, M.P., Pask, A.J., Mullan, D.M., 2012. Physiological breeding I: interdisciplinary approaches to improve crop adaptation. CIMMYT.

R.L. Rorie, L.C. Purcell, M. Mozaffari, D.E. Karcher, C.A. King, M.C. Marsh, D.E. Longer, Association of "greenness" in corn with yield and leaf nitrogen concentration, Agron. J. 103 (2011) 529–535, https://doi.org/10.2134/agronj2010.0296.

J.E. Rutkoski, J. Poland, J.-L. Jannink, M.E. Sorrells, Imputation of unordered markers and the impact on genomic selection accuracy, G3 Bethesda, Md.) 3 (2013) 427–439, https://doi.org/10.1534/g3.112.005363.

W. Sannemann, B.E. Huang, B. Mathew, J. Léon, Multi-parent advanced generation inter-cross in barley: high-resolution quantitative trait locus mapping for flowering time as a proof of concept, Mol. Breed. (2015) 35, https://doi.org/10.1007/s11032-015-0284-7.

Sannemann, W., Lisker, A., Maurer, A., Léon, J., Kazman, E., Cöster, H., Holzapfel, J., Kempf, H., Korzun, V., Ebmeyer, E., Pillen, K., 2018. Adaptive selection of founder segments and epistatic control of plant height in the MAGIC winter wheat population WM-800. BMC genomics 19, 559. ⟨https://doi.org/10.1186/s12864–018-4915–3⟩. 2016. SAS 9.4. SAS Institute Inc., Cary, NC, USA, Cary, NC, USA.

W.-R. Scheible, M. Lauerer, E.-D. Schulze, M. Caboche, M. Stitt, Accumulation of nitrate in the shoot acts as a signal to regulate shoot-root allocation in tobacco+, Plant J. 11 (1997) 671–691, https://doi.org/10.1046/j.1365-313X.1997.11040671.x.

L. Schmidt, K.A. Nagel, A. Galinski, W. Sannemann, K. Pillen, A. Maurer, Unraveling genomic regions controlling root traits as a function of nitrogen availability in the MAGIC wheat population WM-800, Plants (Basel, Switz.) (2022) 11, https://doi.org/10.3390/plants11243520.

R.A. Schofield, Y.-M. Bi, S. Kant, S.J. Rothstein, Over-expression of STP13, a hexose transporter, improves plant growth and nitrogen use in Arabidopsis thaliana seedlings, Plant, Cell Environ. (2009) 271–285, https://doi.org/10.1111/j.1365-3040.2008.01919.x.

D. Sehgal, S. Mondal, L. Crespo-Herrera, G. Velu, P. Juliana, J. Huerta-Espino, S. Shrestha, J. Poland, R. Singh, S. Dreisigacker, Haplotype-based, genome-wide association study reveals stable genomic regions for grain yield in CIMMYT spring bread wheat, Front. Genet. 11 (2020), 589490, https://doi.org/10.3389/fgene.2020.589490.

M.A. Semenov, P.D. Jamieson, P. Martre, Deconvoluting nitrogen use efficiency in wheat: a simulation study, Eur. J. Agron. 26 (2007) 283–294, https://doi.org/10.1016/j.eja.2006.10.009.

L. Serrano, I. Filella, J. Peñuelas, Remote sensing of biomass and yield of winter wheat under different nitrogen supplies, Crop Sci. 40 (2000) 723–731, https://doi.org/10.2135/cropsci2000.403723x.

S. Shi, F.I. Azam, H. Li, X. Chang, B. Li, R. Jing, Mapping QTL for stay-green and agronomic traits in wheat under diverse water regimes, Euphytica (2017) 213, https://doi.org/10.1007/s10681-017-2002-5.

A.K. Shrawat, R.T. Carroll, M. DePauw, G.J. Taylor, A.G. Good, Genetic engineering of improved nitrogen use efficiency in rice by the tissue-specific expression of alanine aminotransferase, Plant Biotechnol. J. (2008) 722–732, https://doi.org/10.1111/j.1467-7652.2008.00351.x.

A. Singh, P. Breja, J.P. Khurana, P. Khurana, Wheat Brassinosteroid-Insensitive1 (TaBRI1) interacts with members of TaSERK gene family and cause early flowering and seed yield enhancement in arabidopsis, PloS One 11 (2016), e0153273, https://doi.org/10.1371/journal.pone.0153273.

M. Stadlmeier, L. Hartl, V. Mohler, Usefulness of a multiparent advanced generation intercross population with a greatly reduced mating design for genetic studies in winter wheat, Front. Plant Sci. 9 (2018) 1825, https://doi.org/10.3389/fpls.2018.01825.

R.J. Staneloni, M.J. Rodriguez-Batiller, J.J. Casal, Abscisic acid, high-light, and oxidative stress down-regulate a photosynthetic gene via a promoter motif not involved in phytochrome-mediated transcriptional regulation, Mol. Plant 1 (2008) 75–83, https://doi.org/10.1093/mp/ssm007.

J. Subira, K. Ammar, F. Álvaro, L.F. Del García Moral, S. Dreisigacker, C. Royo, Changes in durum wheat root and aerial biomass caused by the introduction of the Rht-B1b dwarfing allele and their effects on yield formation, Plant Soil 403 (2016) 291–304, https://doi.org/10.1007/s11104-015-2781-1.

K.N. Suding, S.L. Collins, L. Gough, C. Clark, E.E. Cleland, K.L. Gross, D.G. Milchunas, S. Pennings, Functional- and abundance-based mechanisms explain diversity loss due to N fertilization, Proc. Natl. Acad. Sci. USA 102 (2005) 4387–4392, https://doi.org/10.1073/pnas.0408648102.

S.E. Sultan, Phenotypic plasticity in plants: a case study in ecological development, Evol. Dev. 5 (2003) 25–33, https://doi.org/10.1046/j.1525-142X.2003.03005.x.

E. Triboi, P. Martre, C. Girousse, C. Ravel, A.-M. Triboi-Blondel, Unravelling environmental and genetic relationships between grain yield and nitrogen concentration for wheat, Eur. J. Agron. 25 (2006) 108–118, https://doi.org/10.1016/j.eja.2006.04.004.

M.R. Tuinstra, G. Ejeta, P.B. Goldsbrough, Heterogeneous inbred family (HIF) analysis: a method for developing near-isogenic lines that differ at quantitative trait loci, Theor. Appl. Genet 95 (1997) 1005–1011, https://doi.org/10.1007/s001220050654.

C. Uauy, A. Distelfeld, T. Fahima, A. Blechl, J. Dubcovsky, A NAC Gene regulating senescence improves grain protein, zinc, and iron content in wheat, Science 314 (2006) 1298–1301, https://doi.org/10.1126/science.1133649.

D.A. van Sanford, C.T. MacKown, Cultivar differences in nitrogen remobilization during grain fill in soft red winter wheat 1, Crop Sci. 27 (1987) 295–300, https://doi.org/10.2135/cropsci1987.0011183×002700020035x.

J.J. Vidmar, D. Zhuo, M.Y. Siddiqi, A.D. Glass, Isolation and characterization of HvNRT2.3 and HvNRT2.4, cDNAs encoding high-affinity nitrate transporters from roots of barley, Plant Physiol. 122 (2000) 783–792, https://doi.org/10.1104/pp.122.3.783.

P. Walch-Liu, B.G. Forde, Nitrate signalling mediated by the NRT1.1 nitrate transporter antagonises L-glutamate-induced changes in root architecture, Plant J.: Cell Mol. Biol. (2008) 820–828, https://doi.org/10.1111/j.1365-313X.2008.03443.x.

R. Wang, D. Liu, N.M. Crawford, The Arabidopsis CHL1 protein plays a major role in high-affinity nitrate uptake, Proc. Natl. Acad. Sci. USA 95 (1998) 15134–15139, https://doi.org/10.1073/pnas.95.25.15134.

S. Wang, D. Wong, K. Forrest, A. Allen, S. Chao, B.E. Huang, M. Maccaferri, S. Salvi, S. G. Milner, L. Cattivelli, A.M. Mastrangelo, A. Whan, S. Stephen, G. Barker, R. Wieseke, J. Plieske, M. Lillemo, D. Mather, R. Appels, R. Dolferus, G. Brown-Guedira, A. Korol, A.R. Akhunova, C. Feuillet, J. Salse, M. Morgante, C. Pozniak, M.-C. Luo, J. Dvorak, M. Morell, J. Dubcovsky, M. Ganal, R. Tuberosa, C. Lawley, I. Mikoulitch, C. Cavanagh, K.J. Edwards, M. Hayden, E. Akhunov, Characterization of polyploid wheat genomic diversity using a high-density 90,000 single nucleotide polymorphism array, Plant Biotechnol. J. 12 (2014) 787–796, https://doi.org/10.1111/pbi.12183.

X. Wang, Y. Bian, K. Cheng, H. Zou, S.S.-M. Sun, J.-X. He, A comprehensive differential proteomic study of nitrate deprivation in Arabidopsis reveals complex regulatory networks of plant nitrogen responses, J. Proteome Res. 11 (2012) 2301–2315, https://doi.org/10.1021/pr2010764.

Y. Wang, Q. Yao, Y. Zhang, Y. Zhang, J. Xing, B. Yang, G. Mi, Z. Li, M. Zhang, The role of gibberellins in regulation of nitrogen uptake and physiological traits in maize responding to nitrogen availability, Int. J. Mol. Sci. (2020) 21, https://doi.org/10.3390/ijms21051824.

H.-K. Wong, H.-K. Chan, G.M. Coruzzi, H.-M. Lam, Correlation of ASN2 gene expression with ammonium metabolism in Arabidopsis, Plant Physiol. (2004) 332–338, https://doi.org/10.1104/pp.103.033126.

Y.-H. Xu, R. Liu, L. Yan, Z.-Q. Liu, S.-C. Jiang, Y.-Y. Shen, X.-F. Wang, D.-P. Zhang, Light-harvesting chlorophyll a/b-binding proteins are required for stomatal response to abscisic acid in Arabidopsis, J. Exp. Bot. 63 (2012) 1095–1106, https://doi.org/10.1093/jxb/err315.

T. Yamaya, M. Obara, H. Nakajima, S. Sasaki, T. Hayakawa, T. Sato, Genetic manipulation and quantitative-trait loci mapping for nitrogen recycling in rice, J. Exp. Bot. 53 (2002) 917–925, https://doi.org/10.1093/jexbot/53.370.917.

J. Yan, F. Xiang, P. Yang, X. Li, M. Zhong, R. He, X. Li, W. Peng, X. Liu, X. Zhao, Overexpression of BnGA2ox2, a rapeseed gibberellin 2-oxidase, causes dwarfism and increased chlorophyll and anthocyanin accumulation in Arabidopsis and rapeseed, Plant Growth Regul. 93 (2021) 65–77, https://doi.org/10.1007/s10725-020-00665-6.

S. Yanagisawa, A. Akiyama, H. Kisaka, H. Uchimiya, T. Miwa, Metabolic engineering with Dof1 transcription factor in plants: Improved nitrogen assimilation and growth under low-nitrogen conditions, Proc. Natl. Acad. Sci. USA (2004) 7833–7838, https://doi.org/10.1073/pnas.0402267101.

H. Ye, S. Liu, B. Tang, J. Chen, Z. Xie, T.M. Nolan, H. Jiang, H. Guo, H.-Y. Lin, L. Li, Y. Wang, H. Tong, M. Zhang, C. Chu, Z. Li, M. Aluru, S. Aluru, P.S. Schnable, Y. Yin, RD26 mediates crosstalk between drought and brassinosteroid signalling pathways, Nat. Commun. 8 (2017) 14573, https://doi.org/10.1038/ncomms14573.

L.-P. Yin, P. Li, B. Wen, D. Taylor, J.O. Berry, Characterization and expression of a high-affinity nitrate system transporter gene (TaNRT2.1) from wheat roots, and its evolutionary relationship to other NTR2 genes, Plant Sci. 172 (2007) 621–631, https://doi.org/10.1016/j.plantsci.2006.11.014.

M. Zhang, M. Gao, H. Zheng, Y. Yuan, X. Zhou, Y. Guo, G. Zhang, Y. Zhao, F. Kong, Y. An, S. Li, QTL mapping for nitrogen use efficiency and agronomic traits at the seedling and maturity stages in wheat, Mol. Breed. (2019) 39, https://doi.org/10.1007/s11032-019-0965-8.